Energy Device Applications of Synthesized 1D Polymer Nanomaterials

Long-Biao Huang, [a, c] *Wei Xu,* [a] *and Jianhua Hao,* [a, b,] *

Dr. L. B. Huang, W. Xu, Prof. J. H. Hao,
Department of Applied Physics, The Hong Kong Polytechnic University, Hong Kong, China
E-mail: jh.hao@polyu.edu.hk
Prof. J. H. Hao,
The Hong Kong Polytechnic University Shenzhen Research Institute, Shenzhen 518057, China
Dr. L. B. Huang,
Key Laboratory of Optoelectronic Devices and Systems of Ministry of Education and Guangdong Province, College of Optoelectronic Engineering, Shenzhen University, Shenzhen, 518060, China

Keywords: (1D polymer nanomaterials, nanogenerators, battery, supercapacitor, energy device)

One-dimensional (1D) polymer nanomaterials as emerging materials, such as nanowire, nanotube and nanopillar have attracted extensive attentions in academic and industry. The distinctive, various and tunable structures in nano-scale of 1D polymer nanomaterials present nanointerface, high surface-to-volume ratio and large surface area, which can improve the performance of energy devices. In this review, representative fabrication techniques of 1D polymer nanomaterials are summarized, including electrospinning, template-assisted, template-free and inductively coupled plasma methods. The recent advancements of 1D polymer nanomaterials in energy device applications are demonstrated. Lastly, we will present existing challenges and prospects of 1D polymer nanomaterials for energy device applications.

1. Introduction

The energy crisis, environmental pollution and global warming from traditional fossil fuel have been prompting a number of researchers and institutes to develop new technology, emerging materials and potential applications for green, sustainable and renewable power source.[1-7] Correspondingly, a variety of energy devices, such as nanogenerator, solar cells, lithium ion battery and supercapacitor have been developed to generate and storage electricity.[8-16] As a type of emerging constituent materials in modern electronics, nanomaterials with a range of unique properties and morphology may provide a broad window to enhance the performances for various energy devices, and have been widely investigated during past decades.[2-7, 17-19] Among those nanomaterials, One-dimensional (1D) polymer nanomaterials have attracted a plenty of attentions from both scientists and engineers due to their low-cost, dimension controllable and scale-up fabrication capability.[2-7, 17-19]

Benefited from their high surface-to-volume ratio, and appealing properties in terms of structural, mechanical and electrical aspects, 1D polymer nanomaterials have significant advantages over bulk polymer materials and obvious promotion in functions, which generates an enormous variety of application and achieve great advances in past decades. [20-24] For example, 1D conducting polymer nanomaterials, such as polypyrrole and polyaniline nanowires are considered as electrode materials for supercapacitor.[12, 25-27] 1D insulating polymer nanomaterials, including polytetrafluoroethylene nanowires, Kapton nanowires and others used for nanogenerators, show great electron attraction from metal electrodes, which can

effectively convert mechanical energy into electricity.[28-30] In this review, we will summarize typical 1D polymer nanomaterials for distinct energy devices.

During past decades, some approaches such as electrospinning, template-assisted, and template-free approaches have been extensively utilized to fabricate 1D polymer nanomaterials.[1, 5, 7, 18, 31-33] Besides these methods, inductively coupled plasma technique is intriguing in recent years as a novel and universal method to fabricate 1D polymer nanomaterials.[34-38] However, few reviews have mentioned such an effective fabrication technique of 1D nanomaterials. On the other hand, nanogenerator is a promising energy device for mechanical energy harvesting and self-powered electronics, which has been considered as an alternative to other conventional energy devices (solar cells, lithium ion battery, supercapacitor and so on). Because of its advantages of high converting efficiency, simple fabrication process, expected size and abundant constituent materials choice, nanogenerator shows a great potential of sustainable power source for driving internet of thing and sensor networks.[39] Unfortunately, there has no specific summary containing the application of 1D polymer nanomaterials in nanogenerator device, and providing a comprehensive and updated views on fabricating 1D polymer nanomaterials for energy device applications. Therefore, in this review, we will summarize the representative fabrication techniques of 1D polymer nanomaterials in section 2. Based on the fabrication methods, in section 3, we will highlight the integrations of 1D polymer nanomaterials in nanogenerator, lithium ion battery and supercapacitor. The overview on energy device applications of 1D polymer nanomaterials can offer fundamental

knowledge and comprehend the unique properties of the relevant materials. Finally, we will conclude and comment the advances in section 4. Some challenges and opportunities will be briefly introduced for further research in this field.

2. Fabrication Methods

In principle, a variety of fabrication methods based on "bottom-up" and "top-down" processes play important roles in determining the characteristics, cost and stability of 1D polymer nanomaterials and relevant energy devices.[22, 40-42] **Table 1** summarizes the representative fabrication methods to make 1D polymer nanomaterials. The relative applications of 1D polymer nanomaterials for advanced energy devices include nanogenerator, lithium ion battery and supercapacitor, as shown in **Figure 1**. At present, electrospinning technique is one of most conventional methods which has been widely used to fabricate 1D polymer nanomaterial with a broad range of diameter tailored for various applications such as nanogenerators, lithium ion battery, and supercapacitor. Other approaches, including template-assisted and template-free methods have also been demonstrated and shown amazing performances. The electrospinning technique as a simple and low-cost technique is favourable to fabricating 1D polymer nanomaterials used for lithium ion battery and capacitor when considering the merits of large-scale and fast-speed fabrication. However, most conventional polymer materials for triboelectric nanogenerator such as PTFE and Kapton could not been electrospun into 1D type. Although, inductively coupled plasma as a general method can create 1D polymer nanomaterials on the surface of various polymer films for making nanogenerators, this technique shows limited use in

lithium ion battery and supercapacitor. On the other hand, the template-assisted methods have shown great capability for more classes of energy devices inclucing nanogenerator, lithium ion battery, and supercapacitor. However, comparing with electrospinning, the large-scale capability of template-assisted methods needs further investigation to satisfy the requirements of these energy devices.

2.1. Electrospinning method

As a facile, low-cost, versatile, straightforward and conventional approach, electrospinning is capable of generating ultra-fine micro/nano-fiber with controllable diameter from an electrified liquid. Normally, the basic setup of electrospinning consists of three main parts, including power supply, spinneret and collector. The spinneret with polymer solution or polymer melts is connected with high-voltage power supply. The collector is grounded with/without special design for orientation of 1D polymer nanomaterials. During the electrospinning processes, the polymer solution or polymer melts from a spinneret form a small droplet. Under high electric voltage, a liquid meniscus is charged and stretched to form a thin liquid jet which leads to the formation of micro/nano-fiber. The prototypical instantaneous position of polymer nanomaterials can be schematically illustrated in **Figure 2,** which includes three stages: (1) jet initiation and elongation of charged jet along a straight line; (2) growth of electrical bending instability and further elongation of the jet; (3) solidification of jet into 1D polymer nanomaterials on the collector.[43]

Under electrostatic repulsion of high voltage, the polymer jet is preformatted for the growth of bending instability and further elongation. While the solvent of polymer solution is evaporated, the polymer nanomaterials are deposited on the collector. The formation and the architecture can be controlled by polymer solution properties, applied high voltage and the electrospinning distance between syringe tip and collector and other parameters (humidity, etc.). Attributed to electric force of high voltage, the cone shape of solution droplet is formed and overcome the surface tension of polymer solution and therefore generate solution jet with critical voltage *Vc* given by[44]

$$V_c = 4\frac{H^2}{h^2}\left(ln\left(\frac{2h}{R}\right) - 1.5\right)(1.3\pi R\gamma)(0.09) \quad (1)$$

where *H* is the distance between the syringe needle tip and the collector, *h* is the polymer solution length in syringe, *R* is the out radius of needle, *y* is the surface tension of polymer solution. The influence of electrospinning parameters on the morphology of 1D polymer nanomaterials has systematically been investigated and summarized in **Table 2**.[45-48].

Currently, electrospinning technique has been widely utilized to fabricate 1D polymer nanomaterials, such as nanowires and nanotubes for various classes of energy devices, including lithium ion battery and supercapacitor as discussed in later sections.

2.2. Template-assisted method

Template-assisted method used for 1D polymer nanomaterials mainly includes two classes, namely hard-template and soft-template methods.[49] For hard

template-assisted method, porous templates, such as mesoporous silica, zinc oxide, and anodic aluminum oxide, have been utilized to fabricate 1D polymer nanomaterials, such as polypyrrole (PPy), polyaniline (PAN), poly(*p*-phenylenevinylene) derivatives (PPV) and so on.[24, 49] Especially, the anodic aluminum oxide with controllable diameter of nanochannel through electrochemistry has been proved to be powerful in fabricating 1D polymer nanomaterials.[31, 50] In contrast, soft template-assisted methods involve different block copolymer, surfactant and aggregates, liquid crystal, polymer nanofibers, and biomolecules as templates which can be utilized as sacrifice scaffold to fabricate 1D polymer nanomaterials.[2]

For hard template-assisted method, Steinhart's group pioneered the approach by wetting anodic aluminum and oxidized microporous silicon templates with polymer solution or melts.[51-60] In their earlier studies, 1D polymer nanomaterials were fabricated with feasible and tunable size.[31, 56, 57, 59, 61-66] As shown in **Figure 3a** and **3b**, due to the higher surface energy of porous template, the polystyrene (PS) melt forms a thin wetting film on the surface of nanochannel, and the wall thicknesses can be ranged from 20 to 50 nm. Other materials, such as polytetrafluoroethylene (PTFE) and polymethyl methacrylate (PMMA) can also be fabricated into 1D polymer nanomaterials as shown in Figure 3c and 3d, respectively. By controlling anodic parameter, different nanochannel diameter and depth of anodic aluminum oxide can be achieved, resulting in the controllability of 1D polymer nanomaterials.

Currently, a large variety of polymer and polymer-based composites have been employed to fabricate 1D polymer nanomaterials by template-assist method, such as

PTFE,[67] PS,[68] poly(styrene-block-methyl methacrylate) (PS-b-PMMA),[68] polydimethylsiloxane (PDMS),[29] polypropylene (PP),[69] poly(3-hexylthiophene),[70] etc, as shown in **Figure 4**. The applications of the above 1D polymer nanomaterials can range from chemical sensor electronic to energy devices such as nanogenerators.[50, 67, 69]

2.3. Template-free Method

Template-free methods for preparing 1D polymer nanomaterials mainly include supramolecular self-assembly behaviors of polymer chain in solution or at the interface between solid substrate and liquid solvent,[7, 71, 72] and polymerization methods including electrochemical, interface and dilute polymerization.[18]

Supramolecular self-assembly of polymer chain is promising for making 1D polymer materials for energy devices due to its potential capability for low cost, solution process and large scale fabrication.[2, 7, 17] Self-assembly of polymer chain involves the spontaneous formation of ordered discrete aggregates or higher ordered structures via noncovalent interaction of polymer moleculars.[73-76] A mount of intermolecular interactions such as dipole-dipole, hydrophobic, hydrogen bonding, etc, can influence or direct the self-assembly behaviors. The n-n stacking of 1D semiconductor polymer nanomaterials can be tuned by temperature and solvent during the self-assembly processes. Therefore, by controlling the self-assembly behaviors of polymer chain, 1D polymer nanomaterials can be optimized for energy device applications.[2, 7, 71, 72]

Besides self-assembly method, a range of polymerization methods have been demonstrated by several groups, aiming at creating 1D polymer materials on substrate

for energy devices.[23, 25, 42] For example, 1D conducting PPy nanowires can be deposited on substrate by electrochemical polymerization. The mechanism of electrochemical polymerization involves three steps: (1) electrodeposition of PPy film, (2) formation of O_2 nanobubbles and hydroxyl radicals and overoxidation of polymer monomer, and (3) growth of 1D PPy nanowires.[77, 78] Similarly, the 1D PAN nanowires can be fabricated on the surface of electrode for energy devices by electrochemical polymerization.[79-81] For example, through electrodeposition at high current density, the PAN nanoparticles as nucleation sites were created on the substrate. Following decrement of current density, further nucleation for growth of 1D PAN nanowire occurs.[81] Dilute polymerization method has been developed to prepare 1D polymer nanomaterials on the surface of various conducting and insulating substrates as shown in **Figure 5**. The mechanism of dilute polymerization involves the occurrence of heterogeneous nucleation on the surface of materials. Consequently, active nucleation centers are generated and minimize the interfacial energy barrier for the following growth of PAN. Due to the precipitation of PAN induced by the formation of polyaniline nanofiber in bulk solution, 1D PAN nanofibers can grow from the active nucleation centers.[18]

2.4. Inductively Coupled Plasma

Recently, inductively coupled plasma as a large-scale, one-step, clean fabrication method of 1D polymer nanomaterials on the surface of polymer is appealing since the technique was presented by Wang's group.[82] Subsequently, a series of 1D polymer nanomaterials arrays based on various polymers, including

(poly(3,4-ethylenedioxythiophene) poly(styrenesulfonate)) (PEDOT:PSS), PPy, poly(1-methyoxy-2-propyl acetate) (SU8), polyvinylidene difluoride (PVDF), PMMA, PS, poly(2-methoxy-5-2'-ethylhexyloxy)-(1,4-phenylenevinylene) (MEH-PPV), have been fabricated on the surface of polymer film with large scale, as shown in **Figure 6**. The fabrication mechanism of 1D polymer nanomaterials by inductively coupled plasma involves etching reaction between polymer surface and plasma, which contains chemical wet etching and physical ion-beam milling. General gas components utilized to create plasma and radicals include Ar, O_2 and CF_4. By controlling the vacuum pressure, gas flow rate, and power, aligned 1D polymer nanomaterials can be controllably fabricated on the surface of polymer.

3. Energy Device Applications

When the dimension of material decreases down to nanoscale range, the properties of nanomaterials may significantly differ from their bulk counterparts.[83, 84] Accordingly, 1D polymer nanomaterials have unique physical and chemical properties compared with bulk polymer materials, leading to a number of novel applications, especially, in energy device.[13, 21, 22, 42, 49] With the growing threat of energy crises, developing energy device with decent performance are gaining importance in various fields. Generally, there are two types of energy devices, namely the energy harvesting device, such as nanogenerator and solar cells etc., and the energy stroage device, such as supercapacitor and lithium ion battery. The following sections will discuss the utilization of 1D polymer nanomaterials in representative energy devices, including nanogenerator, lithium ion battery and supercapacitor.

3.1. Nanogenerator

Since Wang's group firstly invented triboelectric nanogenerators (TENGs) in 2012, TENGs as a new generation of nanogenerators have achieved great progress from academic and industry pools due to their potential applications, such as energy harvesting and self-powered systems.[15, 16, 33] Based on the triboelectric and electrostatic effect between different materials, TENGs could be utilized to harvest ambient energies such as body motion energy, vibration energy, wind energy and large-scale blue energy.[39, 85] Through optimizating devices, TENGs can combine with other energy device and form hybrid cell such as hybrid electromagnetic and TENG, hybrid triboelectric-piezoelectric/pyroelectric nanogenerator, hybrid solar cell and TENG, hybrid thermoelectric cell and TENG, hybrid electrochemical cell and TENG.[39] A broad classes of self-powered sensors for human-machine interface, vibration and biomedical monitoring have also been developed.[39, 86]

Polymer materials, as essential components in TENGs, have been widly used in four different working modes (contact-separation mode, lateral sliding mode, single-electrode mode, and freestanding triboelectric-layer mode).[39] To improve the performance of TENG, 1D polymer nanomaterials with an diameter from around 20 nm to 400 nm have been fabricated on the surface of polymer film to increase the contact area between polymer film and counter-materials. Inductively coupled plasma and template-assisted methods are the extensively employed fabrication approaches of 1D polymer nanomaterials on the surface of polymer film in TENG.[36, 38, 69, 87-90]

1D polymer nanomaterials such as PTFE,[28, 34, 35, 38, 91, 92] fluorinated ethylene propylene (FEP),[88, 90, 93-95] poly vinyl chloride (PVC),[37] Kapton,[36, 87, 96] with around 20 nm to 200 nm fabricated by inductively coupled plasma have been demonstrated in nanogenerators. For example, Zhu et al. fabricated the 1D Kapton nanowires with ~ 80 nm on the surface of Kapton film by inductively coupled plasma to convert ambient energy, such as vibration and random displacements/deformation, into electricity.[97] The output power of TENG with 1D Kapton nanowires can achieve 31.2 mW/cm^3 at a maximum open-circuit voltage of 110 V as shown in **Figure 7**. The prepared device can be used as a power source for pulse electrodeposition of micro/nanocrystalline silver structure. Similarly, Hu etc. also took advantage of inductively coupled plasma to fabricate 1D Kapton nanowires of about 100 nm on Kapton film for TENGs as shown in **Figure 8**.[98] The optimized 3D spiral structure was integrated into a TENG to harvest ambient energy with the power of 2.76 W/m^2 on a load of 6 Mn. Interestingly, the fabricated device as self-powered active sensors can identify multiple position as multichannel and location of vibration source with an error of less than 6%.

Besides 1D Kapton nanomaterials, 1D PTFE nanowires as active materials have also been presented for TENG. For example, Zheng et al. demonstrated an implantable TENG with 1D PTFE nanowire with ~ 100 nm fabricated by inductively coupled plasma for *in vivo* biomechanical energy harvesting as shown in **Figure 9**.[92] . Driven by the heartbeat, the performance of energy device shows an obvious improvement, compared with *in vivo* output performance of a reported biomechanical

energy conversion devices which can be utilized not only to power implantable medical devices but also possibly to fabricate a self-powered, wireless healthcare monitoring system. Ma et al. have also illustrated the application of 1D PTFE nanowire in implantable triboelectric active sensor.[28] The results presented that the device can continuously monitor physiological and pathological signs with about 99% accuracy in monitoring heart rate and show proof-of-concept demonstration of implantable biomedical sensor. Decoration of 1D PTFE nanowires on active layer in TENGs has also been used to monitor cardiovascular system and applied in throat-attached anti-interference voice recognition.[99] Those results show that the 1D polymer nanomaterials on the surface of polymer films can provide large contact area with counter-materials, such as metal electrode or polymer film. To further increase contact area, 1D polymer nanomaterails with smaller diameter could be achieved to enhance the output performance of TENGs.

Moreover, other approaches, such as electrospinning, template-assisted, pattern transfer and self-assembly, have been considered as effective methods to create 1D polymer nanomaterials for TENG. For example, Wang et al. demonstrated that the electrospun PVDF nanowires can be the active polymer materials for scavenging mechanical and thermal energies.[100] As shown in **Figure 10a** and **10b**, the electrospun PVDF nanowires with 200-500 nm can be deposited on the surface of ITO electrode and form polymer composite with PDMS. The prepared device as hybridized nanogenerators can be applied to harvest mechanical and thermal energies by triboelectric-piezoelectric-pyroelectric effects. Under a compressed/stretched stain

on the device, the polarization change in PVDF nanowires can generate piezoelectricity. Meanwhile, the electron transfer between nylon film and PVDF nanowires induces the generation of electricity due to their different triboelectric polarities. The temperature change on PVDF film can lead to the electric dipoles oscillation which results in an electron flow.

Template-assisted methods for 1D polymer nanomaterials such as nanopillar and nanowire have been successfully applied to nanogenerators based on various polymers, including PP,[69] PDMS,[29, 89] PTFE,[30, 67] etc. Recently, Song et al. developed a novel sleeping monitoring system based on nanogenerator with PP nanopillar of about 700 nm fabricated by the AAO template-assisted technique as shown in **Figure 11**.[69] By increasing the temperature to 180 °C for 10 min, PP melts were absorbed into the nanochannels of AAO templates. After removing templates, the PP nanopillars with a length of 1.5 μm were fabricated for TENGs, which can increase the open-circuit voltage with more than doubled to 55 V due to enhanced contact area between the electrode and PP film. As aforementioned, 1D polymer nanomaterials with smaller diameter can achieve higher contact area. Therefore, the template-assisted method can be employed to fabricate 1D polymer nanomaterials with smaller diameter, as the diameter of nanohole in the AAO can be precisely controlled.

For self-assembly and pattern-transfer technique utilized in nanogenerators, the self-assembly of block copolymer has been investigated by Lee's group.[101] By thermal and solvent vapor annealing, polystyrene-block-polydimethylsiloxane

(PS-b-PDMS) performs self-assembly and forms nanodots, nanogrates and nanomeshes on the surface of device for TENGs as shown in **Figure 12**. The results confirmed that the nanostructure on the surface of device significantly influenced the performance of TENGs. Pattern transfer technique as an effective and reusable approach has been demonstrated by several groups for fabrication of micropyramids[102-104] and nanowires[105, 106] for nanogenerators. Our group transfered the 1D PDMS microwires from DVD disc to enhance the contact areas between polymer and electrode in nanogenerators.[107] By combinating with magnetic composite, we developed a novel noncontact TENG which can harvest mechanical energy without direct contact with external objects as shown in **Figure 13**.

3.2. Lithium Ion Battery

Lithium ion batteries (LIBs) as one of secondary batteries have many attractive and interesting advantages, such as high energy density, low maintenance, and relatively low self-discharge.[1, 5, 6, 19, 32, 107] The basic elements of a LIB contain an anode, polymer porous film as separator, a cathode, and electrolyte with dissociated lithium salts.[1, 5, 6, 19, 32] Excellent lithium storage behavior in anode and cathode materials can lead to high performance LIB with great capacity, excellent efficiency, and long cycling life.[19, 32] To enhance the performance of LIB, 1D nanomaterials such as nanofiber and nanotube have been widely utilized to fabricate basic LIBs materials such as anode and cathode materials. Comparing with commercial carbon graphite, 1D carbon nanofibers/nanotubes have shown unique properties such as high surface area for electrolyte and short Li-ion insertion/extraction distance.[40, 107, 108] Meanwhile,

1D carbon nanofibers/nanotubes have also presented the advantages in anti-aggregation and formation stability as electrode materials, comparing with other carbon nanomaterials.[21, 109]

As the most popular fabrication technique of 1D nanomaterials for LIB, electrospinning can be adopted to design component materials (anodes, cathodes, and separators). The obvious advantages of electrospun materials for LIBs comparing with traditional carbon graphite, including large surface area for electrolyte, strain relaxation during electrochemical cycling and short Li^+-ion insertion/extraction distance, have been demonstrated by several groups and proven that they can improve the performance of LIBs.[109-114] Especially, 1D carbon nanofibers frequently utilized for LIBs can be fabricated as anode and cathode materials after carbonization of electrospun 1D polymer nanomaterials such as PAN,[115, 116] and poly(vinyl alcohol) (PVA).[117, 118] Kim et al. have demonstrated the conversion of electrospun 1D PAN nanofiber into carbon nanofiber at 1000 °C.[110] Due to the high electrical conductivity between carbon nanofibers, the prepared LIBs can achieve 450 $mAhg^{-1}$ which was obviously enhanced comparing with others. By controlling the morphology of 1D PAN nanofiber through electrospinning, the capacity and rate capability of LIBs can be further improved due to the optimized surface area or Li-ion insertion/extraction distance.[119-121] By incorporating different filler into the 1D PAN nanofibers during electrospinning processes, the rate property and capacity of LIBs can be improved due to the appearance of active filler.[122, 123] For example, the Fe precursor was electrospun and incorporated into 1D PAN nanofibers and functioned as catalyst for

graphitization of carbon nanofiber and sacrificial phases for formation of nanopores on carbon nanofibers.[122] After removing the Fe_3C particles by chemical etching, amount of nanopores were created on carbon nanofiber, leading to high capacity retention and excellent rate capability of prepared LIBs. Hwang et al. incorporated commercially available Si nanoparticles into 1D PAN nanofiber (~ 800 nm) by utilization of electrospinning with dual nozzle.[109] Because of the high Li^+ ion storage of Si nanoparticle and core-shell structure in 1D carbon fibers as shown **Figure 14**, the prepared LIBs presented excellent performance including high gravimetric capability with 1384 $mAhg^{-1}$, excellent discharging rate capability with 5 min keeping 721 $mAhg^{-1}$, and very stable capacitor without loss after 300 times charging/discharging. The high performance of the prepared LIBs might be attributed to the unique core-shell structure that the Si nanoparticles were encapsulated into 1D carbon nanofiber, leading to solvation of pulverization, vulnerable contact between Si and carbon conductors, and solid-electrolyte interphase.

Besides the conversion into carbon nanofiber, 1D polymer nanomaterials can also be utilized as scarification materials to form metal oxide nanofiber which can perform intercalation/de-intercalation reaction or conversion reaction as anode materials for LIBs. Recently, Xu et al. fabricated porous anode materials with $Li_4Ti_5O_{12}$ (LTO)/C nanofibers (PLTO/C) for LIBs as shown in **Figure 15a**.[124] 1D PVP/LTO precursor nanofiber with about 300 nm was fabricated by electrospinning precursor solution of lithium acetylacetonate (LAA), titanium isopropoxide (TTIP) and poly(vinyl pyrrolidone) (PVP) in the mixture of ethanol and acetic acid. After heated at 800 °C

in H_2/Ar (H_2, 5%), the precursors in nanofiber were converted into crystalline LTO and carbon. The carbon concentration was controlled by temperature (350 °C) in air. The final porous structure of PLTO/C nanofiber was formed at secondary calcination process as shown in Figure 15b, and the element distribution of nanofiber was homogeneous in Figure 15c. The LIBs fabricated by PLTO/C nanofibers show great performance with high reversible capacity, exhibiting ultrahigh cycling rates and superior cycling stability.

Nowadays, a variety of transition metal oxide nanofibers including M_xO_y (M = Mn, Fe, Co, Ni, Cu, etc.) with conversion reaction for LIBs have been demonstrated via the conversion of 1D polymer nanomaterials through the electrospinning technique.[20, 125] Because of high capacity, low cost and environmental friendliness, iron oxides nanofibers such as Fe_2O_3 and Fe_3O_4 nanofibers have been fabricated as anode materials by conversion of electrospun 1D polymer nanomaterials.[126-128] Recently, Cho et al. fabricated "bubble-nanorod composites", where the bubble-nanorod-structured Fe_2O_3-C composite nanofibers were achieved by post-treatment of electrospun 1D $Fe(acac)_3$/PAN nanofibers as shown in **Figure 16a**.[126] TEM images in Figure 16b and 16c presented the morphology of Fe_2O_3-C composite and bare Fe_2O_3 hollow nanofibers (~ 200 nm) after post-treatment at high temperature. The prepared LIBs demonstrate excellent performance with discharge capacity of 812 $mAhg^{-1}$ after 300 cycles at a current density of 1 A/g and 84% capacity retention from the second cycle, as shown in Figure 16d and 16c. Other metal oxide nanofibers/nanotubes such as cobalt oides,[129, 130] manganese oxides,[131]

nikel oxides,[132] copper oxides,[133], tungsten oxides[134] and mixed transition metal oxide,[135, 136] have successfully been prepared by the utilization of electrospinning technique.

Besides the anode materials from 1D polymer nanomaterials, cathode materials based on lithium-containing metal oxides (i.e. $LiCoO_2$, $LiFePO_4$, and $LiMn_2O_4$) have been prepared through scarification of 1D polymer nanomaterials.[137] For example, hollow $LiMn_2O_4$ nanofibers with ~ 500 nm have been fabricated after conversion of 1D PVP/precursor nanofiber at high temperature in **Figure 17a** to **17d**.[137] the LIBs based on hollow $LiMn_2O_4$ nanofibers present very stable discharge capacity (97% of initial discharge capacity) after 100 cycles. As shown in Figure 17e, the rate performance of LIBs demonstrated the well battery characteristics that the reversible capacities of 119, 117, 111, 97 and 56 $mAhg^{-1}$ are achieved at the current rates of 1, 2, 4, 8, and 16 C, respectively. The cyclability at a high current rate of 1 C for about 1250 cycles shows no obvious difference in Figure 17f.

The electrospun 1D polymer nanomaterials can be utilized as template or carbon source for fabrication of transition metal oxide nanofibers which have shown promising results.[138, 139] For example, the vanadium pentoxide (V_2O_5) has attracted amount of concerns due to high theoretical capacity.[138, 139] As shown in **Figure 18**, Wang et al. presented the electrospinning of PVP and vanadium(IV) acetylacetone to fabricate porous V_2O_5 nanotubes, hierarchical V_2O_5 nanofibers, and single-crystalline V_2O_5 nanobelts which can be used as cathode materials for LIBs and show a highly reversible capacity, excellent cycling performance, and good rate capacity.[140] The

PVP plays an important role as scarification template and carbon source of CO_2 for formation of V_2O_5 nanomaterials. During the decomposition of PVP matrix, the diffusion of CO_2 leads to the creation of V_2O_5 with different morphologies. The results shows that the V_2O_5 nanotubes have better performance due to the porous structure which shortens the diffusion distance of Li^+ ion and increases the contact areas of electrode-electrolyte for high Li^+ ion flux. Therefore, the LIBs based on V_2O_5 nanotubes can achieve a high power density of 40.2 kW kg^{-1} and high energy density of 201 Wh kg^{-1}.

The electrospun 1D polymer nanomaterials can not only be employed as anode and cathode materials, but also be membrane separator for LIBs between the cathode and anode.[141-143] The membrane separators fabricated by 1D polymer nanomaterials have high porosities, large specific surface areas, and interconnected porous structures for the transportation of Li^+ ion, resulting into improved ionic conductivity and thermal stability.[141-143] Correspondingly, a series of 1D polymer nanomaterials such as polyimide (PI), PAN, PVDF and their copolymer have been developed for LIBs separator.[141-143] Besides of the excellent thermal and electrochemical stabilities, 1D poly(vinylidene fluoride-co-chlorotrifluoroethylene) (PVDF-CTFE) nanofiber shows good affinity with electrolyte in LIBs.[144] As shown in **Figure 19**, by optimization of electrospinning parameters, PVDF-CTFE nanofibers (230 ± 38 nm) were fabricated to form membrane separator. Due to the extensive interaction between PVDF-CTFE nanofibers and electrolyte, the nanofibers become swollen as shown in Figure 19b. The performance of prepared LIBs presents high conductivity at different

temperatures and excellent mechanical stability. Additionally, electrospun PAN and PI nanofibers membranes also possess excellent flexibility and rigidity for LIBs.[145-147]

3.3 Supercapacitor

Nowadays, supercapacitor as one of most commonly used energy devices is also presented with rapid progress.[4, 21-23, 148] To increase the energy density, charge-discharge rate and elongate the cycle life of supercapacitor, a variety of 1D polymer nanomaterials have been utilized for two types of supercapacitor: electric double layers capacitor (EDLC) and pseudocapacitors.[4, 10-12, 148] Mechanism of EDLC is mainly based on charge accumulation in the electric double layer between the electrode/electrolyte. While, the fast and reversible redox reaction or Faradic charge transfer reaction at the surface of transition metal oxide and conducting polymer play critical role in the mechanism of pseudocapacitors. The 1D polymer nanomaterials for supercapacitor are mainly fabricated by electrospinning, template-assisted, and template-free methods. Similar to the LIBs, the 1D polymer nanomaterial can also function as template or carbon source for conversion into other usable nanomaterials in supercapacitor. Those polymers include: PAN, PI, PVP, PVA, polybenzimidazole (PBI), phenolic resin, PVDF, cellulose etc.[14, 22, 149]

Recently, the electrospinning technique has been proved to be an effective approach which creates carbon nanofiber network or textile with high surface area, nanopores, high conductivity for EDLC.[4, 10, 12, 148] To increase the porosity of carbon

nanofiber, several approaches have been applied for electrospun 1D polymer nanomaterials such as steam or chemical activations.[13] Cui's group reported a novel bamboo-like carbon nanofibers by incorporating SiO_2 nanoparticles into the 1D PAN nanofibers as shown in **Figure 20**.[13] After carbonization and etching SiO_2 nanoparticles away by HF, 1D PAN nanofibers were converted into carbon nanofiber (~ 200 nm) with a well-balanced macro-, meso-, and microporosity as shown in Figure 20d. In addition to the improved porosity, the periodic distribution of bamboo-like holes in carbon nanofibers provides mechanical stability under different deformation. Therefore, the supercapacitor electrodes based on the novel bamboo-like carbon nanofiber show excellent mechanical properties such as flexibility. After even being folded for three times, the electrode still keeps its initial property. Furthermore, high stability of prepared electrode keeps 100% of initial capacitance after 5000 cycles at 10 A/g illustrated in Figure 20f.

For a long time, the use of traditional conducting polymer in pseudocapacitor is limited due to their low practical capacitance and poor cyclic stability during charge-discharge processes. To overcome these shortcoming, some strategies, such as varied morphology and microstructure of conducting polymer, conducting polymer composites and electrolyte with wide electrochemical window, have been researched. Especially, 1D conducting polymer nanomaterials with high contact area for electrolyte and short transport path length for electrons and ions have shown great potential.[8, 9, 26, 150-152] The 1D conducting polymer nanomaterials such as PAN, PPy,

poly(3,4-ethylenedioxythiophene) (PEDOT) and others have been synthesized as well by template-assisted and template-free methods for pseudocapacitors.[4, 23, 152, 153]

The most used templates for preparation of 1D conducting polymer nanomaterials include AAO, particle track-etched membrane (PTM), block copolymer self-assembly film.[31, 153, 154] For example, AAO template-assisted method was used to fabricate 1D PEDOT/MnO_2 or RuO_2 nanowires for supercapacitor as shown in **Figure 21**.[24, 154] The PEDOT shell thickness and nanowire length can be controlled by applied voltage. The prepared uniform nanowires with the diameter of around 250 nm were evident as excellent materials for electrochemical supercapacitor with high specific capacitance (210 to 185 F/g) and current density (5 to 25 mA/cm^2) in Figure 21e. 1D PAN nanowires fabricated by AAO template-assisted synthesis also provides a porous material for supercapacitor that the capacitance values can reach up to 700 F/g at a charge-discharge rate of 5 A/g.[155]

For template-free methods, the electrochemical and dilute polymerizations are reported to prepare 1D conducting polymer nanowires such as PPy and PAN for supercapacitor.[77, 78, 156, 157] By changing the processes of polymerization, the length of 1D conducting polymer nanowires are controlled as shown in **Figure 22a-c**.[156] The capacitance of PPy nanowires can achieve to be 566 F/g at a discharge current density of 1.1 A/g and keep 70 % of capacitance after hundreds of charge-discharge cycles. Comparing with PPy nanowires arrays, the disordered PPy nanowire networks and film are only 414 and 378 F/g. The research results reveal that the 1D PPy nanowires provide larger contact area and shorter penetrating path for ions. 1D PAN

nanowires have been reported to be prepared on a variety of conducting substrates by template-free method as shown in **Figure 23**.[25] The narrow diameter and vertical orientation of 1D PAN nanowire make it a good candidate material for supercapacitor that the capacitance of 1D PAN nanowire is around 950 F/g and can keep around 780 F/g at the charge-discharge current density of 40 A/g. The positive results of 1D PPy and PAN nanowires for supercapacitor prove that the ordered or aligned 1D conducting polymer nanomaterials can significantly enhance the performance of supercapacitor by reducing the ionic diffusion path and enhancement of ionic motion.

Recently, the combination of 1D conducting polymer nanomaterials with 2D materials has been reported to enhance the performance of supercapacitor.[27, 152, 158] As shown in **Figure 24a** and **24b**, through the heterogeneous nucleation, 1D PAN nanowires with the diameter of about 20 nm can be synthesized and further form aligned nanowire arrays on the surface of 2D graphene oxide (GO).[152] The novel nanomaterials as supercapacitor materials show higher capacitance (555 F/g at a discharge current density of 0.2 A/g) than the random PAN nanowire networks (298 F/g), and better stability as shown in Figure 24c and 24d.

4. Summary and outlook

In this review, we summarize the representative fabrication approaches of 1D polymer nanomaterials for advanced energy device including nanogenerator, lithium ion battery, and supercapacitor. The latest results have revealed that the unique properties of 1D polymer nanomaterial, such as high surface area, excellent nanointerface, and chemical conversion capability, have been widely utilized to

enhance the performance of energy devices. For example, 1D polymer nanowires on the surface of polymer film provide larger contact area between contact materials which can improve the energy conversion efficiency from mechanical energy into electricity. The 1D carbon nanofibers originated from 1D polymer nanomaterials show excellent properties such as high conductivity and large surface area for improvement in perfomance of lithium ion battery and supercapacitor. These results confirm the capability and versatility of 1D polymer nanomaterials for diverse applications in advanced energy devices.

In the majority of the aforementioned examples, it should be mentioned that the inductively coupled plasma and template-assisted methods have shown obvious advantages to fabricate 1D polymer nanomaterials with controllable diameter and length for nanogenerators. However, how to improve these methods with increased efficiency, high speed, low-cost and large-scale capability still needs to be noticed. On the other hand, 1D nanomaterials converted by electrospun 1D polymer nanomaterials need to be further optimized as well to achieve various morphologies and porous structure which can improve the mass loading of LIB electrodes. Especially, the electrospun 1D polymer nanomaterials with a diameter less than 50 nm are still very challenging to meet the requirment of LIBs and supercapacitor. Meanwhile, the electrospun 1D polymer nanomaterials with loading materials such as filler and precursor also need further improvement and optimization. We believe that the combination of electrospinning technique with other fabrication methods could be an ideal approach to overcome above barriers. Besides these 1D polymer

nanomaterials formed directly on the surface of energy devices, it should be mentioned that for powder-like 1D nanomaterials, advanced spin coating, screen printing and injet printing techniques could be utilized to introduce the nanostructure into the energy devcies. In future studies, the investigation of fundamental mechanism and materials chemistry for 1D polymer nanomaterials fabricated by these methods are still open issues. Further development relies on gaining comprehensive understanding of the fundamental polymer physics, polymer chemistry and relative theoretical models. It is expected that the development of 1D polymer nanomaterials will promote the performance of advanced energy device and show great potentials in a variety of applications.

Acknowledgements

The research was financially supported by the grants from National Natural Science Foundation of China (Grant No. 11474241) and Research Grants Council of Hong Kong (GRF No. PolyU 153004/14P).

Received: ((will be filled in by the editorial staff))
Revised: ((will be filled in by the editorial staff))
Published online: ((will be filled in by the editorial staff))

References

[1]. Sun, Y. M.; Liu, N. A.; Cui, Y., *Nat Energy* **2016,** *1*.

[2]. Kim, Y.; Cook, S.; Tuladhar, S. M.; Choulis, S. A.; Nelson, J.; Durrant, J. R.; Bradley, D. D. C.; Giles, M.; Mcculloch, I.; Ha, C. S.; Ree, M., *Nature Materials* **2006,** *5* (3), 197-203.

[3]. Li, G.; Shrotriya, V.; Huang, J. S.; Yao, Y.; Moriarty, T.; Emery, K.; Yang, Y., *Nature Materials* **2005,** *4* (11), 864-868.
[4]. Simon, P.; Gogotsi, Y., *Nature Materials* **2008,** *7* (11), 845-854.
[5]. Chan, C. K.; Peng, H. L.; Liu, G.; McIlwrath, K.; Zhang, X. F.; Huggins, R. A.; Cui, Y., *Nature Nanotechnology* **2008,** *3* (1), 31-35.
[6]. Liu, N.; Lu, Z. D.; Zhao, J.; McDowell, M. T.; Lee, H. W.; Zhao, W. T.; Cui, Y., *Nature Nanotechnology* **2014,** *9* (3), 187-192.
[7]. Chen, H. Y.; Hou, J. H.; Zhang, S. Q.; Liang, Y. Y.; Yang, G. W.; Yang, Y.; Yu, L. P.; Wu, Y.; Li, G., *Nat Photonics* **2009,** *3* (11), 649-653.
[8]. Wang, K.; Zou, W. J.; Quan, B. G.; Yu, A. F.; Wu, H. P.; Jiang, P.; Wei, Z. X., *Advanced Energy Materials* **2011,** *1* (6), 1068-1072.
[9]. Yin, Z. G.; Zheng, Q. D., *Advanced Energy Materials* **2012,** *2* (2), 179-218.
[10]. Zhai, Y. P.; Dou, Y. Q.; Zhao, D. Y.; Fulvio, P. F.; Mayes, R. T.; Dai, S., *Advanced Materials* **2011,** *23* (42), 4828-4850.
[11]. Frackowiak, E.; Beguin, F., *Carbon* **2001,** *39* (6), 937-950.
[12]. Bose, S.; Kuila, T.; Mishra, A. K.; Rajasekar, R.; Kim, N. H.; Lee, J. H., *Journal of Materials Chemistry* **2012,** *22* (3), 767-784.
[13]. Sun, Y. M.; Sills, R. B.; Hu, X. L.; Seh, Z. W.; Xiao, X.; Xui, H. H.; Luo, W.; Jin, H. Y.; Xin, Y.; Li, T. Q.; Zhang, Z. L.; Zhou, J.; Cai, W.; Huang, Y. H.; Cui, Y., *Nano Letters* **2015,** *15* (6), 3899-3906.
[14]. Zhang, B. A.; Kang, F. Y.; Tarascon, J. M.; Kim, J. K., *Progress in Materials Science* **2016,** *76*, 319-380.
[15]. Zi, Y. L.; Niu, S. M.; Wang, J.; Wen, Z.; Tang, W.; Wang, Z. L., *Nature Communications* **2015,** *6*.
[16]. Zi, Y. L.; Wang, J.; Wang, S. H.; Li, S. M.; Wen, Z.; Guo, H. Y.; Wang, Z. L., *Nature Communications* **2016,** *7*.
[17]. Peet, J.; Kim, J. Y.; Coates, N. E.; Ma, W. L.; Moses, D.; Heeger, A. J.; Bazan, G. C., *Nature Materials* **2007,** *6* (7), 497-500.
[18]. Chiou, N. R.; Lui, C. M.; Guan, J. J.; Lee, L. J.; Epstein, A. J., *Nature Nanotechnology* **2007,** *2* (6), 354-357.
[19]. Lin, D.; Liu, Y.; Cui, Y., *Nature Nanotechnology* **2017,** *12* (3), 194-206.
[20]. Goriparti, S.; Miele, E.; De Angelis, F.; Di Fabrizio, E.; Zaccaria, R. P.; Capiglia, C., *J Power Sources* **2014,** *257*, 421-443.
[21]. Jung, J. W.; Lee, C. L.; Yu, S.; Kim, I. D., *Journal of Materials Chemistry A* **2016,** *4* (3), 703-750.
[22]. Inagaki, M.; Yang, Y.; Kang, F. Y., *Advanced Materials* **2012,** *24* (19), 2547-2566.
[23]. Chiou, N. R.; Epstein, A. J., *Advanced Materials* **2005,** *17* (13), 1679-1683.
[24]. Cho, S. I.; Lee, S. B., *Accounts of Chemical Research* **2008,** *41* (6), 699-707.
[25]. Wang, K.; Huang, J. Y.; Wei, Z. X., *J Phys Chem C* **2010,** *114* (17), 8062-8067.
[26]. Hui, N.; Chai, F. L.; Lin, P. P.; Song, Z. L.; Sun, X. T.; Li, Y. N.; Niu, S. Y.; Luo, X. L., *Electrochim Acta* **2016,** *199*, 234-241.
[27]. Ouyang, A.; Cao, A. Y.; Hu, S.; Li, Y. H.; Xu, R. Q.; Wei, J. Q.; Zhu, H. W.; Wu, D. H., *Acs Applied Materials & Interfaces* **2016,** *8* (17), 11179-11187.

[28]. Ma, Y.; Zheng, Q.; Liu, Y.; Shi, B. J.; Xue, X.; Ji, W. P.; Liu, Z.; Jin, Y. M.; Zou, Y.; An, Z.; Zhang, W.; Wang, X. X.; Jiang, W.; Xu, Z. Y.; Wang, Z. L.; Li, Z.; Zhang, H., *Nano Letters* **2016,** *16* (10), 6042-6051.
[29]. Zhang, H. L.; Yang, Y.; Hou, T. C.; Su, Y. J.; Hu, C. G.; Wang, Z. L., *Nano Energy* **2013,** *2* (5), 1019-1024.
[30]. Lin, Z. H.; Cheng, G.; Li, X. H.; Yang, P. K.; Wen, X. N.; Wang, Z. L., *Nano Energy* **2015,** *15*, 256-265.
[31]. Steinhart, M.; Wendorff, J. H.; Greiner, A.; Wehrspohn, R. B.; Nielsch, K.; Schilling, J.; Choi, J.; Gosele, U., *Science* **2002,** *296* (5575), 1997-1997.
[32]. Wu, H.; Chan, G.; Choi, J. W.; Ryu, I.; Yao, Y.; McDowell, M. T.; Lee, S. W.; Jackson, A.; Yang, Y.; Hu, L. B.; Cui, Y., *Nature Nanotechnology* **2012,** *7* (5), 309-314.
[33]. Fan, F. R.; Tian, Z. Q.; Wang, Z. L., *Nano Energy* **2012,** *1* (2), 328-334.
[34]. Li, Z. L.; Chen, J.; Guo, H. Y.; Fan, X.; Wen, Z.; Yeh, M. H.; Yu, C. W.; Cao, X.; Wang, Z. L., *Advanced Materials* **2016,** *28* (15), 2983-2991.
[35]. Yang, Y.; Zhang, H. L.; Wang, Z. L., *Advanced Functional Materials* **2014,** *24* (24), 3745-3750.
[36]. Chen, X. Y.; Pu, X.; Jiang, T.; Yu, A. F.; Xu, L.; Wang, Z. L., *Advanced Functional Materials* **2017,** *27* (1).
[37]. Du, W. M.; Han, X.; Lin, L.; Chen, M. X.; Li, X. Y.; Pan, C. F.; Wang, Z. L., *Advanced Energy Materials* **2014,** *4* (11).
[38]. Yang, W. Q.; Chen, J.; Zhu, G.; Yang, J.; Bai, P.; Su, Y. J.; Jing, Q. S.; Cao, X.; Wang, Z. L., *Acs Nano* **2013,** *7* (12), 11317-11324.
[39]. Wang, Z. L.; Chen, J.; Lin, L., *Energy & Environmental Science* **2015,** *8* (8), 2250-2282.
[40]. Chen, J.; Cheng, F. Y., *Accounts of Chemical Research* **2009,** *42* (6), 713-723.
[41]. Aravindan, V.; Sundaramurthy, J.; Kumar, P. S.; Lee, Y. S.; Ramakrishna, S.; Madhavi, S., *Chemical Communications* **2015,** *51* (12), 2225-2234.
[42]. Wang, K.; Wu, H. P.; Meng, Y. N.; Wei, Z. X., *Small* **2014,** *10* (1), 14-31.
[43]. Reneker, D. H.; Yarin, A. L., *Polymer* **2008,** *49* (10), 2387-2425.
[44]. Xu, H.; Reneker, D. H., *Acs Sym Ser* **2006,** *918*, 21-35.
[45]. Deitzel, J. M.; Kleinmeyer, J.; Harris, D.; Tan, N. C. B., *Polymer* **2001,** *42* (1), 261-272.
[46]. Theron, S. A.; Zussman, E.; Yarin, A. L., *Polymer* **2004,** *45* (6), 2017-2030.
[47]. Beachley, V.; Wen, X. J., *Mat Sci Eng C-Bio S* **2009,** *29* (3), 663-668.
[48]. Fong, H.; Chun, I.; Reneker, D. H., *Polymer* **1999,** *40* (16), 4585-4592.
[49]. Mijangos, C.; Hernández, R.; Martín, J., *Progress in Polymer Science* **2016,** *54-55*, 148-182.
[50]. Huang, L. B.; Zhou, Y.; Han, S. T.; Yan, Y.; Zhou, L.; Chen, W., *Small* **2014**.
[51]. Grimm, S.; Schwirn, K.; Goring, P.; Knoll, H.; Miclea, P. T.; Greiner, A.; Wendorff, J. H.; Wehrspohn, R. B.; Gosele, U.; Steinhart, M., *Small* **2007,** *3* (6), 993-1000.
[52]. Feng, C. L.; Zhong, X. H.; Steinhart, M.; Caminade, A. M.; Majoral, J. P.; Knoll, W., *Small* **2008,** *4* (5), 566-571.
[53]. Hillebrand, R.; Muller, F.; Schwirn, K.; Lee, W.; Steinhart, M., *Acs Nano* **2008,**

2 (5), 913-920.
[54]. Lee, W.; Schwirn, K.; Steinhart, M.; Pippel, E.; Scholz, R.; Gosele, U., *Nature Nanotechnology* **2008,** *3* (4), 234-239.
[55]. Wang, Y.; Gosele, U.; Steinhart, M., *Nano Letters* **2008,** *8* (10), 3548-3553.
[56]. Duran, H.; Steinhart, M.; Butt, H. J.; Floudas, G., *Nano Letters* **2011,** *11* (4), 1671-1675.
[57]. Pulamagatta, B.; Yau, M. Y. E.; Gunkel, I.; Thurn-Albrecht, T.; Schroter, K.; Pfefferkorn, D.; Kressler, J.; Steinhart, M.; Binder, W. H., *Advanced Materials* **2011,** *23* (6), 781-+.
[58]. Alexandris, S.; Papadopoulos, P.; Sakellariou, G.; Steinhart, M.; Butt, H. J.; Floudas, G., *Macromolecules* **2016,** *49* (19), 7400-7414.
[59]. Franz, C.; Lange, F.; Golitsyn, Y.; Hartmann-Azanza, B.; Steinhart, M.; Krutyeva, M.; Saalwachter, K., *Macromolecules* **2016,** *49* (1), 244-256.
[60]. Yao, Y.; Sakai, T.; Steinhart, M.; Butt, H. J.; Floudas, G., *Macromolecules* **2016,** *49* (16), 5945-5954.
[61]. Kriha, O.; Zhao, L. L.; Pippel, E.; Gosele, U.; Wehrspohn, R. B.; Wendorff, J. H.; Steinhart, M.; Greiner, A., *Advanced Functional Materials* **2007,** *17* (8), 1327-1332.
[62]. Duran, H.; Gitsas, A.; Floudas, G.; Mondeshki, M.; Steinhart, M.; Knoll, W., *Macromolecules* **2009,** *42* (8), 2881-2885.
[63]. Maiz, J.; Schafer, H.; Rengarajan, G. T.; Hartmann-Azanza, B.; Eickmeier, H.; Haase, M.; Mijangos, C.; Steinhart, M., *Macromolecules* **2013,** *46* (2), 403-412.
[64]. Duran, H.; Hartmann-Azanza, B.; Steinhart, M.; Gehrig, D.; Laquai, F.; Feng, X. L.; Mullen, K.; Butt, H. J.; Floudas, G., *Acs Nano* **2012,** *6* (11), 9359-9365.
[65]. Chen, X.; Steinhart, M.; Hess, C.; Gosele, U., *Advanced Materials* **2006,** *18* (16), 2153-+.
[66]. Kriha, O.; Gring, P.; Milbradt, M.; Azgarwal, S.; Steinhart, M.; Wehrspohn, R.; Wendorff, J. H.; Greiner, A., *Chemistry of Materials* **2008,** *20* (3), 1076-1081.
[67]. Lin, Z. H.; Cheng, G.; Lee, S.; Pradel, K. C.; Wang, Z. L., *Advanced Materials* **2014,** *26* (27), 4690-+.
[68]. Wang, Y.; Goesele, U.; Steinhart, M., *Chemistry of Materials* **2008,** *20* (2), 379-381.
[69]. Song, W. X.; Gan, B. H.; Jiang, T.; Zhang, Y.; Yu, A. F.; Yuan, H. T.; Chen, N.; Sun, C. W.; Wang, Z. L., *Acs Nano* **2016,** *10* (8), 8097-8103.
[70]. Huang, L. B.; Xu, Z. X.; Chen, X. F.; Tian, W.; Han, S. T.; Zhou, Y.; Xu, J. J.; Yang, X. B.; Roy, V. A. L., *Acs Appl Mater Inter* **2014,** *6* (15), 11874-11881.
[71]. Kim, J. S.; Lee, J. H.; Park, J. H.; Shim, C.; Sim, M.; Cho, K., *Advanced Functional Materials* **2011,** *21* (3), 480-486.
[72]. Chen, D. A.; Nakahara, A.; Wei, D. G.; Nordlund, D.; Russell, T. P., *Nano Letters* **2011,** *11* (2), 561-567.
[73]. Kim, F. S.; Ren, G. Q.; Jenekhe, S. A., *Chemistry of Materials* **2011,** *23* (3), 682-732.
[74]. Lehn, J. M., *P Natl Acad Sci USA* **2002,** *99* (8), 4763-4768.
[75]. Lehn, J. M., *Science* **2002,** *295* (5564), 2400-2403.

[76]. Whitesides, G. M.; Grzybowski, B., *Science* **2002,** *295* (5564), 2418-2421.
[77]. Debiemme-Chouvy, C., *Electrochem Commun* **2009,** *11* (2), 298-301.
[78]. Li, M.; Wei, Z. X.; Jiang, L., *Journal of Materials Chemistry* **2008,** *18* (19), 2276-2280.
[79]. Ye, Y.-J.; Huang, Z.-H.; Song, Y.; Geng, J.-W.; Xu, X.-X.; Liu, X.-X., *Electrochim Acta* **2017,** *240*, 72-79.
[80]. Hui, N.; Chai, F.; Lin, P.; Song, Z.; Sun, X.; Li, Y.; Niu, S.; Luo, X., *Electrochim Acta* **2016,** *199*, 234-241.
[81]. Liang, L.; Liu, J.; Windisch, C. F.; Exarhos, G. J.; Lin, Y. H., *Angewandte Chemie-International Edition* **2002,** *41* (19), 3665-3668.
[82]. Fang, H.; Yuan, D. J.; Guo, R.; Zhang, S.; Han, R. P. S.; Das, S.; Wang, Z. L., *Acs Nano* **2011,** *5* (2), 1476-1482.
[83]. Xia, Y. N.; Yang, P. D.; Sun, Y. G.; Wu, Y. Y.; Mayers, B.; Gates, B.; Yin, Y. D.; Kim, F.; Yan, Y. Q., *Adv Mater* **2003,** *15* (5), 353-389.
[84]. Hochbaum, A. I.; Chen, R. K.; Delgado, R. D.; Liang, W. J.; Garnett, E. C.; Najarian, M.; Majumdar, A.; Yang, P. D., *Nature* **2008,** *451* (7175), 163-U5.
[85]. Zhang, X. S.; Han, M. D.; Meng, B.; Zhang, H. X., *Nano Energy* **2014**.
[86]. Wang, Z. L., *Acs Nano* **2013,** *7* (11), 9533-9557.
[87]. Hu, Y. F.; Yang, J.; Niu, S. M.; Wu, W. Z.; Wang, Z. L., *Acs Nano* **2014,** *8* (7), 7442-7450.
[88]. Wang, S. H.; Niu, S. M.; Yang, J.; Lin, L.; Wang, Z. L., *Acs Nano* **2014,** *8* (12), 12004-12013.
[89]. Yang, Y.; Zhang, H. L.; Liu, Y.; Lin, Z. H.; Lee, S.; Lin, Z. Y.; Wong, C. P.; Wang, Z. L., *Acs Nano* **2013,** *7* (3), 2808-2813.
[90]. Yang, Y.; Zhu, G.; Zhang, H. L.; Chen, J.; Zhong, X. D.; Lin, Z. H.; Su, Y. J.; Bai, P.; Wen, X. N.; Wang, Z. L., *Acs Nano* **2013,** *7* (10), 9461-9468.
[91]. Yang, Y.; Zhou, Y. S.; Zhang, H. L.; Liu, Y.; Lee, S. M.; Wang, Z. L., *Advanced Materials* **2013,** *25* (45), 6594-6601.
[92]. Zheng, Q.; Zhang, H.; Shi, B. J.; Xue, X.; Liu, Z.; Jin, Y. M.; Ma, Y.; Zou, Y.; Wang, X. X.; An, Z.; Tang, W.; Zhang, W.; Yang, F.; Liu, Y.; Lang, X. L.; Xu, Z. Y.; Li, Z.; Wang, Z. L., *ACS Nano* **2016,** *10* (7), 6510-6518.
[93]. Li, Z. L.; Chen, J.; Zhou, J. J.; Zheng, L.; Pradel, K. C.; Fan, X.; Guo, H. Y.; Wen, Z.; Yeh, M. H.; Yu, C. W.; Wang, Z. L., *Nano Energy* **2016,** *22*, 548-557.
[94]. Guo, H.; Wen, Z.; Zi, Y.; Yeh, M. H.; Wang, J., *Advanced Energy* . **2015**.
[95]. Li, S. M.; Wang, S. H.; Zi, Y. L.; Wen, Z.; Lin, L.; Zhang, G.; Wang, Z. L., *Acs Nano* **2015,** *9* (7), 7479-7487.
[96]. Lin, L.; Wang, S. H.; Xie, Y. N.; Jing, Q. S.; Niu, S. M.; Hu, Y. F.; Wang, Z. L., *Nano Letters* **2013,** *13* (6), 2916-2923.
[97]. Zhu, G.; Pan, C. F.; Guo, W. X.; Chen, C. Y.; Zhou, Y. S.; Yu, R. M.; Wang, Z. L., *Nano Letters* **2012,** *12* (9), 4960-4965.
[98]. Hu, Y. F.; Yang, J.; Jing, Q. S.; Niu, S. M.; Wu, W. Z.; Wang, Z. L., *Acs Nano* **2013,** *7* (11), 10424-10432.
[99]. Yang, J.; Chen, J.; Su, Y. J.; Jing, Q. S.; Li, Z. L.; Yi, F.; Wen, X. N.; Wang, Z. N.; Wang, Z. L., *Advanced Materials* **2015,** *27* (8), 1316-1326.

[100]. Wang, S. H.; Wang, Z. L.; Yang, Y., *Advanced Materials* **2016,** *28* (15), 2881-2887.

[101]. Jeong, C. K.; Baek, K. M.; Niu, S.; Nam, T. W.; Hur, Y. H.; Park, D. Y.; Hwang, G. T.; Byun, M.; Wang, Z. L.; Jung, Y. S.; Lee, K. J., *Nano Letters* **2014,** *14* (12), 7031-7038.

[102]. Meng, B.; Tang, W.; Too, Z. H.; Zhang, X. S.; Han, M. D.; Liu, W.; Zhang, H. X., *Energy & Environmental Science* **2013,** *6* (11), 3235-3240.

[103]. Dhakar, L.; Pitchappa, P.; Tay, F. E. H.; Lee, C., *Nano Energy* **2016,** *19*, 532-540.

[104]. Tang, W.; Tian, J. J.; Zheng, Q.; Yan, L.; Wang, J. X.; Li, Z.; Wang, Z. L., *Acs Nano* **2015,** *9* (8), 7867-7873.

[105]. Huang, L. B.; Bai, G. X.; Wong, M. C.; Yang, Z. B.; Xu, W.; Hao, J. H., *Advanced Materials* **2016,** *28* (14), 2744-2751.

[106]. Huang, L.-b.; Xu, W.; Bai, G.; Wong, M.-C.; Yang, Z.; Hao, J., *Nano Energy* **2016,** *30*, 36-42.

[107]. Cui, L. F.; Yang, Y.; Hsu, C. M.; Cui, Y., *Nano Letters* **2009,** *9* (9), 3370-3374.

[108]. Cheng, F. Y.; Liang, J.; Tao, Z. L.; Chen, J., *Advanced Materials* **2011,** *23* (15), 1695-1715.

[109]. Hwang, T. H.; Lee, Y. M.; Kong, B. S.; Seo, J. S.; Choi, J. W., *Nano Letters* **2012,** *12* (2), 802-807.

[110]. Kim, C.; Yang, K. S.; Kojima, M.; Yoshida, K.; Kim, Y. J.; Kim, Y. A.; Endo, M., *Advanced Functional Materials* **2006,** *16* (18), 2393-2397.

[111]. Wang, L.; Yu, Y.; Chen, P. C.; Chen, C. H., *Scripta Mater* **2008,** *58* (5), 405-408.

[112]. Wang, L.; Yu, Y.; Chen, P. C.; Zhang, D. W.; Chen, C. H., *J Power Sources* **2008,** *183* (2), 717-723.

[113]. Ji, L. W.; Medford, A. J.; Zhang, X. W., *Journal of Materials Chemistry* **2009,** *19* (31), 5593-5601.

[114]. Yu, Y.; Gu, L.; Zhu, C. B.; van Aken, P. A.; Maier, J., *Journal of the American Chemical Society* **2009,** *131* (44), 15984-15985.

[115]. Gu, S. Y.; Ren, J.; Vancso, G. J., *Eur Polym J* **2005,** *41* (11), 2559-2568.

[116]. Ji, L. W.; Zhang, X. W., *Nanotechnology* **2009,** *20* (15).

[117]. Fan, X.; Zou, L.; Zheng, Y. P.; Kang, F. Y.; Shen, W. C., *Electrochem Solid St* **2009,** *12* (10), A199-A201.

[118]. Zou, L.; Gan, L.; Lv, R. T.; Wang, M. X.; Huang, Z. H.; Kang, F. Y.; Shen, W. C., *Carbon* **2011,** *49* (1), 89-95.

[119]. Wu, Y. Z.; Reddy, M. V.; Chowdari, B. V. R.; Ramakrishna, S., *Acs Applied Materials & Interfaces* **2013,** *5* (22), 12175-12184.

[120]. Ji, L. W.; Yao, Y. F.; Toprakci, O.; Lin, Z.; Liang, Y. Z.; Shi, Q.; Medford, A. J.; Millns, C. R.; Zhang, X. W., *J Power Sources* **2010,** *195* (7), 2050-2056.

[121]. Peng, Y. T.; Lo, C. T., *J Electrochem Soc* **2015,** *162* (6), A1085-A1093.

[122]. Zhang, B.; Xu, Z. L.; He, Y. B.; Abouali, S.; Garakani, M. A.; Heidari, E. K.; Kang, F. Y.; Kim, J. K., *Nano Energy* **2014,** *4*, 88-96.

[123]. Hwang, T. H.; Lee, Y. M.; Kong, B.-S.; Seo, J.-S.; Choi, J. W., *Nano Letters* **2012,** *12* (2), 802-807.

[124]. Xu, H. H.; Hu, X. L.; Sun, Y. M.; Luo, W.; Chen, C. J.; Liu, Y.; Huang, Y. H., *Nano Energy* **2014,** *10*, 163-171.

[125]. Yuan, C. Z.; Wu, H. B.; Xie, Y.; Lou, X. W., *Angewandte Chemie-International Edition* **2014,** *53* (6), 1488-1504.

[126]. Cho, J. S.; Hong, Y. J.; Kang, Y. C., *Acs Nano* **2015,** *9* (4), 4026-4035.

[127]. Zhang, X.; Liu, H. H.; Petnikota, S.; Ramakrishna, S.; Fan, H. J., *Journal of Materials Chemistry A* **2014,** *2* (28), 10835-10841.

[128]. Qin, X. Y.; Zhang, H. R.; Wu, J. X.; Chu, X. D.; He, Y. B.; Han, C. P.; Miao, C.; Wang, S. A.; Li, B. H.; Kang, F. Y., *Carbon* **2015,** *87*, 347-356.

[129]. Zhang, M.; Yan, F. L.; Tang, X.; Li, Q. H.; Wang, T. H.; Cao, G. Z., *Journal of Materials Chemistry A* **2014,** *2* (16), 5890-5897.

[130]. Chen, M. H.; Xia, X. H.; Yin, J. H.; Chen, Q. G., *Electrochim Acta* **2015,** *160*, 15-21.

[131]. Park, S. H.; Lee, W. J., *J Power Sources* **2015,** *281*, 301-309.

[132]. Yan, X. Y.; Tong, X. L.; Wang, J.; Gong, C. W.; Zhang, M. G.; Liang, L. P., *Materials Letters* **2014,** *136*, 74-77.

[133]. Sahay, R.; Kumar, P. S.; Aravindan, V.; Sundaramurthy, J.; Ling, W. C.; Mhaisalkar, S. G.; Ramakrishna, S.; Madhavi, S., *J Phys Chem C* **2012,** *116* (34), 18087-18092.

[134]. Lee, J.; Jo, C.; Park, B.; Hwang, W.; Lee, H. I.; Yoon, S.; Lee, J., *Nanoscale* **2014,** *6* (17), 10147-10155.

[135]. Hwang, S. M.; Kim, S. Y.; Kim, J. G.; Kim, K. J.; Lee, J. W.; Park, M. S.; Kim, Y. J.; Shahabuddin, M.; Yamauchi, Y.; Kim, J. H., *Nanoscale* **2015,** *7* (18), 8351-8355.

[136]. Qiao, H.; Luo, L.; Chen, K.; Fei, Y. Q.; Cui, R. R.; Wei, Q. F., *Electrochim Acta* **2015,** *160*, 43-49.

[137]. Jayaraman, S.; Aravindan, V.; Kumar, P. S.; Ling, W. C.; Ramakrishna, S.; Madhavi, S., *Chemical Communications* **2013,** *49* (59), 6677-6679.

[138]. Yu, D. M.; Chen, C. G.; Xie, S. H.; Liu, Y. Y.; Park, K.; Zhou, X. Y.; Zhang, Q. F.; Li, J. Y.; Cao, G. Z., *Energy & Environmental Science* **2011,** *4* (3), 858-861.

[139]. Yue, Y.; Liang, H., *Advanced Energy Materials* **2017**.

[140]. Wang, H. G.; Ma, D. L.; Huang, Y.; Zhang, X. B., *Chem-Eur J* **2012,** *18* (29), 8987-8993.

[141]. Zhou, X. H.; Yue, L. P.; Zhang, J. J.; Kong, Q. S.; Liu, Z. H.; Yao, J. H.; Cui, G. L., *J Electrochem Soc* **2013,** *160* (9), A1341-A1347.

[142]. Zhai, Y. Y.; Wang, N.; Mao, X.; Si, Y.; Yu, J. Y.; Al-Deyab, S. S.; El-Newehy, M.; Ding, B., *Journal of Materials Chemistry A* **2014,** *2* (35), 14511-14518.

[143]. Miao, Y. E.; Zhu, G. N.; Hou, H. Q.; Xia, Y. Y.; Liu, T. X., *J Power Sources* **2013,** *226*, 82-86.

[144]. Croce, F.; Focarete, M. L.; Hassoun, J.; Meschini, I.; Scrosati, B., *Energy*

& Environmental Science **2011,** *4* (3), 921-927.
[145]. Cho, T. H.; Sakai, T.; Tanase, S.; Kimura, K.; Kondo, Y.; Tarao, T.; Tanaka, M., *Electrochem Solid St* **2007,** *10* (7), A159-A162.
[146]. Cho, T. H.; Tanaka, M.; Onishi, H.; Kondo, Y.; Nakamura, T.; Yamazaki, H.; Tanase, S.; Sakai, T., *J Power Sources* **2008,** *181* (1), 155-160.
[147]. Kim, J. M.; Kim, C.; Yoo, S.; Kim, J. H.; Kim, J. H.; Lim, J. M.; Park, S.; Lee, S. Y., *Journal of Materials Chemistry A* **2015,** *3* (20), 10687-10692.
[148]. Zhang, L. L.; Zhao, X. S., *Chem Soc Rev* **2009,** *38* (9), 2520-2531.
[149]. Peng, S. J.; Li, L. L.; Lee, J. K. Y.; Tian, L. L.; Srinivasan, M.; Adams, S.; Ramakrishna, S., *Nano Energy* **2016,** *22*, 361-395.
[150]. Chmiola, J.; Yushin, G.; Gogotsi, Y.; Portet, C.; Simon, P.; Taberna, P. L., *Science* **2006,** *313* (5794), 1760-1763.
[151]. Largeot, C.; Portet, C.; Chmiola, J.; Taberna, P. L.; Gogotsi, Y.; Simon, P., *Journal of the American Chemical Society* **2008,** *130* (9), 2730-+.
[152]. Xu, J. J.; Wang, K.; Zu, S. Z.; Han, B. H.; Wei, Z. X., *Acs Nano* **2010,** *4* (9), 5019-5026.
[153]. Qiu, H. J.; Zhai, J.; Li, S. H.; Jiang, L.; Wan, M. X., *Advanced Functional Materials* **2003,** *13* (12), 925-928.
[154]. Liu, R.; Lee, S. B., *Journal of the American Chemical Society* **2008,** *130* (10), 2942-2943.
[155]. Cao, Y.; Mallouk, T. E., *Chemistry of Materials* **2008,** *20* (16), 5260-5265.
[156]. Huang, J. Y.; Wang, K.; Wei, Z. X., *Journal of Materials Chemistry* **2010,** *20* (6), 1117-1121.
[157]. Conway, B. E., *J Electrochem Soc* **1991,** *138* (6), 1539-1548.
[158]. Khosrozadeh, A.; Darabi, M. A.; Xing, M.; Wang, Q., *Acs Applied Materials & Interfaces* **2016,** *8* (18), 11379-11389.
[159]. Gitsas, A.; Yameen, B.; Lazzara, T. D.; Steinhart, M.; Duran, H.; Knoll, W., *Nano Letters* **2010,** *10* (6), 2173-2177.
[160]. Jang, Y. J.; Jang, Y. H.; Han, S. B.; Khatua, D.; Hess, C.; Ahn, H.; Ryu, D. Y.; Shin, K.; Park, K. W.; Steinhart, M.; Kim, D. H., *Acs Nano* **2013,** *7* (2), 1573-1582.
[161]. Suzuki, Y.; Duran, H.; Steinhart, M.; Kappl, M.; Butt, H. J.; Floudas, G., *Nano Letters* **2015,** *15* (3), 1987-1992.
[162]. Chen, D.; Zhao, W.; Russell, T. P., *Acs Nano* **2012,** *6* (2), 1479-1485.
[163]. Lu, X. H.; Hlaing, H.; Nam, C. Y.; Yager, K. G.; Black, C. T.; Ocko, B. M., *Chemistry of Materials* **2015,** *27* (1), 60-66.
[164]. Xin, H.; Kim, F. S.; Jenekhe, S. A., *Journal of the American Chemical Society* **2008,** *130* (16), 5424-+.
[165]. Chen, J.; Zhu, G.; Yang, W. Q.; Jing, Q. S.; Bai, P.; Yang, Y.; Hou, T. C.; Wang, Z. L., *Advanced Materials* **2013,** *25* (42), 6094-6099.
[166]. Zuo, W. W.; Zhu, M. F.; Yang, W.; Yu, H.; Chen, Y. M.; Zhang, Y., *Polym Eng Sci* **2005,** *45* (5), 704-709.
[167]. Rangarajan, S.; Mehta, K.; Chase, G. G., *Air Filtration Conference, Proceedings* **1999**, 177-185.
[168]. Demir, M. M.; Yilgor, I.; Yilgor, E.; Erman, B., *Polymer* **2002,** *43* (11),

3303-3309.
[169]. Meechaisue, C.; Dubin, R.; Supaphol, P.; Hoven, V. P.; Kohn, J., *J Biomat Sci-Polym E* **2006,** *17* (9), 1039-1056.
[170]. Thompson, C. J.; Chase, G. G.; Yarin, A. L.; Reneker, D. H., *Polymer* **2007,** *48* (23), 6913-6922.
[171]. Zhang, C. X.; Yuan, X. Y.; Wu, L. L.; Han, Y.; Sheng, J., *Eur Polym J* **2005,** *41* (3), 423-432.
[172]. Katti, D. S.; Robinson, K. W.; Ko, F. K.; Laurencin, C. T., *J Biomed Mater Res B* **2004,** *70b* (2), 286-296.

Figure list

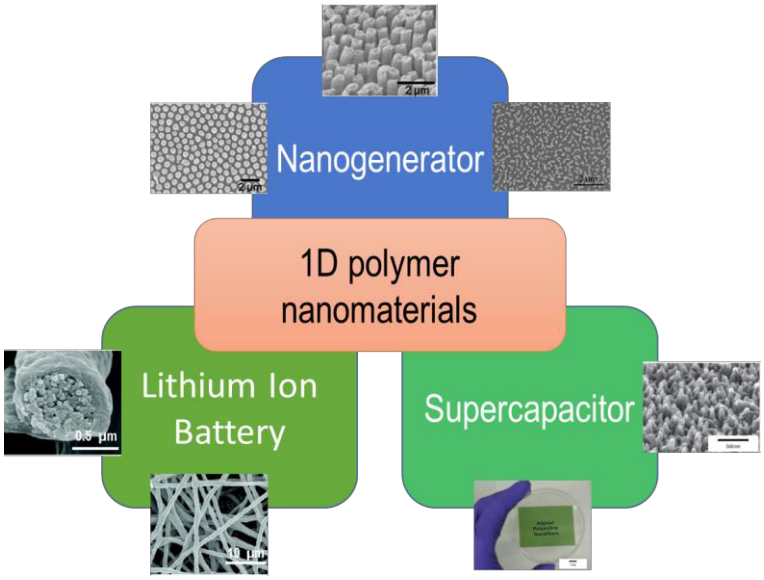

Figure. 1 The applications of 1D polymer nanomaterials for nanogenerators, lithium ion battery, and supercapacitor. The inset SEM images present the relative 1D polymer nanomaterials.

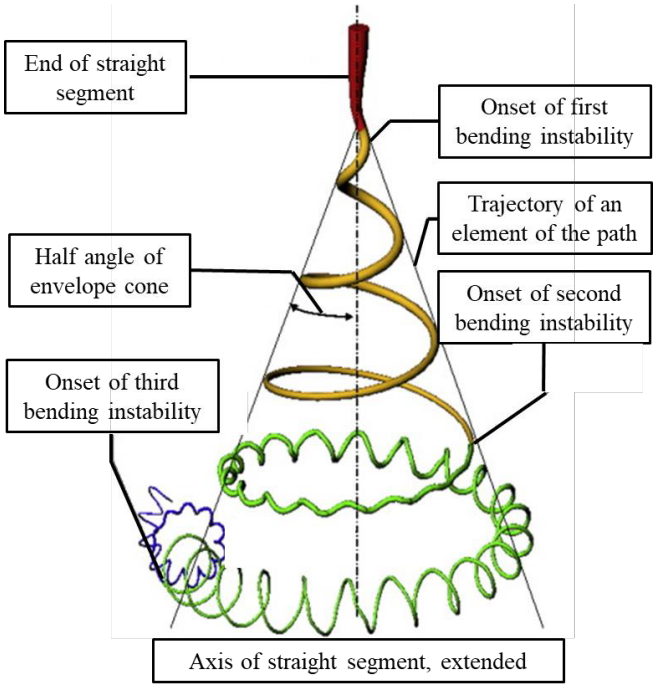

Figure. 2 Schematic illustration of prototypical instantaneous position of 1D polymer nanomaterials during electrospinning. Reproduced with permission.[43] Copyright 2008, Elesiver.

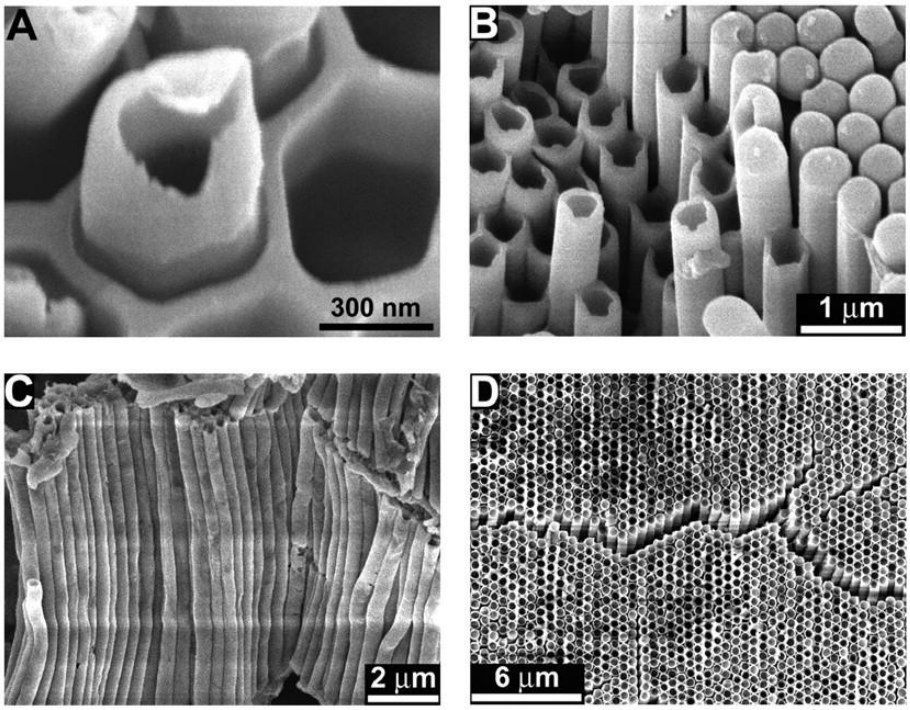

Figure. 3 SEM images of 1D polymer nanotubes fabricated by template-assisted method. (a) Damaged tip of 1D PS nanotube with molecular weight of ~ 850,000 g/mol. (b) Ordered PS nanotube arrays after removing template. (c) 1D PTFE nanotube array after removing template. (d) PMMA tubes with long-range hexagonal order after removing template. Reproduced with permission.[31] Copyright 2002, AAAS.

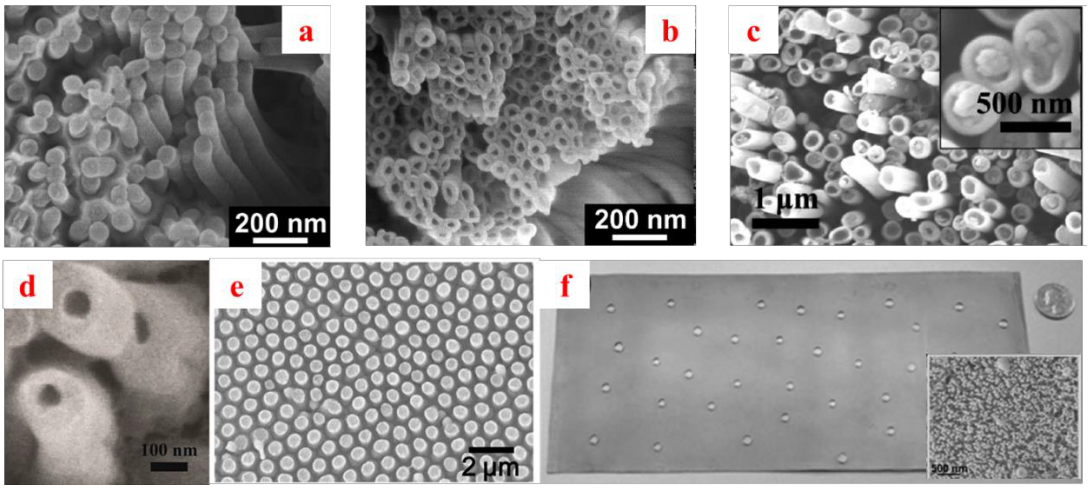

Figure. 4 SEM images of 1D polymer nanomaterials fabricated by template-assisted method. (a) SEM image of PS-*b*-PMMA nanofibers.[68] (b) SEM image of PS nanotubes.[68] (c) FESEM image of PE nanotubes decorated with AgNPs on the top. (d) FESEM image of the RR-P3HT nanotubes.[70] (e) SEM images of PP nanopillar arrays.[69] (f) Photograph of a large- sized PTFE thin film (13 cm × 33 cm) with uniform superhydrophobicity.[67] Inset shows SEM image with higher magnification of PTFE nanowires. Reproduced with permission.[67] Copyright 2014, John Wiley & Sons. Reproduced with permission.[68] Copyright 2008, American Chemical Society. Reproduced with permission.[69] Copyright 2016, American Chemical Society. Reproduced with permission.[70] Copyright 2014, John Wiley & Sons.

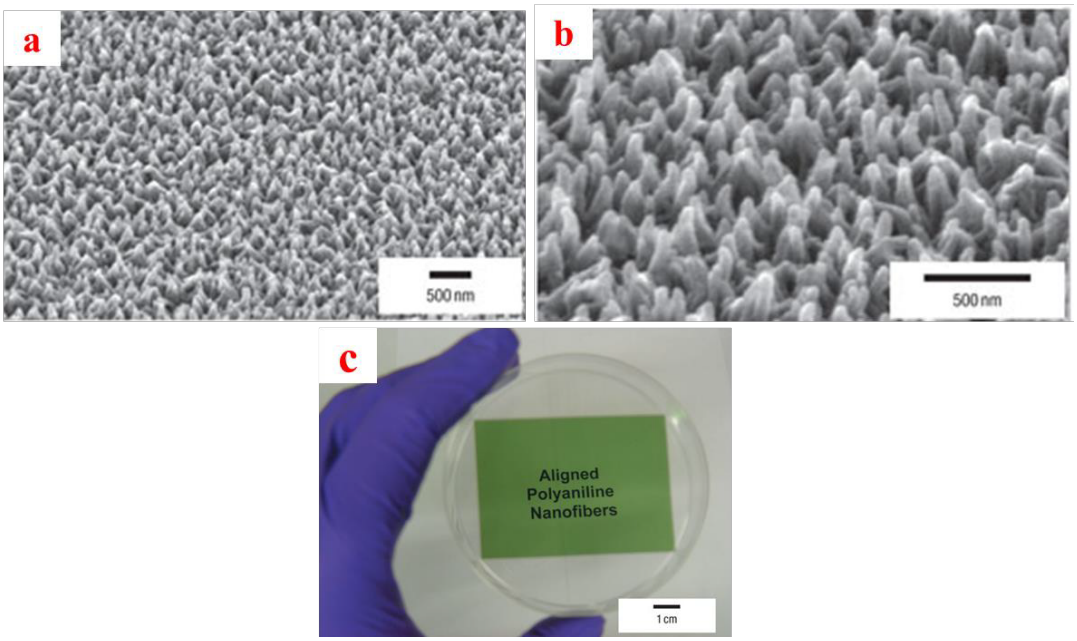

Figure. 5 (a) and (b) SEM images of PAN nanowires at tilted view, high magnification. (c) The large scale film with PAN nanowires which have been re-doped by 1 M $HCl_{(aq)}$ at ambient temperature. DC conductivity is in the range of ~70-75 S cm^{-1}. Reproduced with permission.[18] Copyright 2007, Nature.

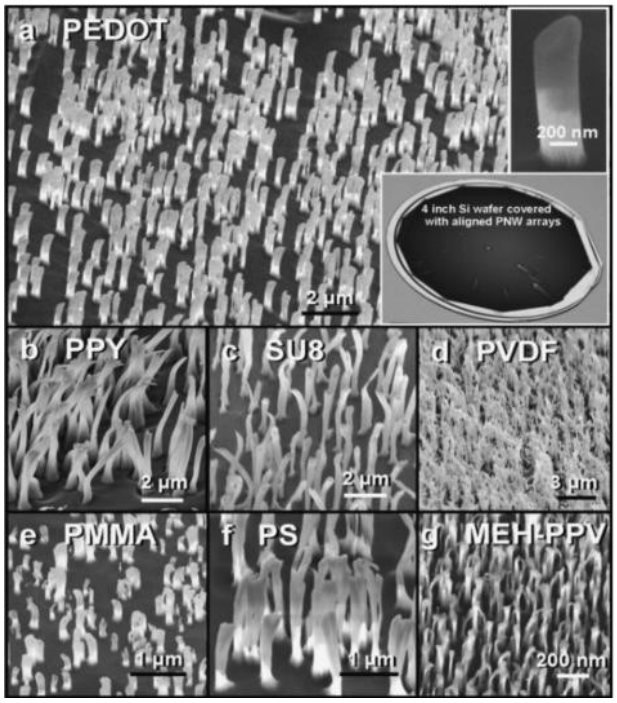

Figure. 6 A series of SEM images demonstrating successful nanowire array formation for a variety of conductive and non-conductive polymers using the presented technique. (a) PEDOT:PSS (poly(3,4-ethylenedioxythiophene) poly(styrenesulfonate)), (b) PPy (polypyrrole), (c) SU8 (1-methyoxy-2-propyl acetate), (d) PVDF (Polyvinylidene difluoride), (e) PMMA (poly(methyl-methacrylate)), (f) PS (polystyrene), (g) MEH-PPV (poly(2-methoxy-5-2'-ethylhexyloxy)-1,4-phenylenevinylene). The top inset in a) is a single PEDOT:PSS NW showing a uniform diameter along its length. The bottom inset in a) is an optical image of a 4 inch wafer that is fully covered with aligned PNWs (darker area), fabricated by a one-step process. Reproduced with permission.[82] Copyright 2011, American Chemical Society.

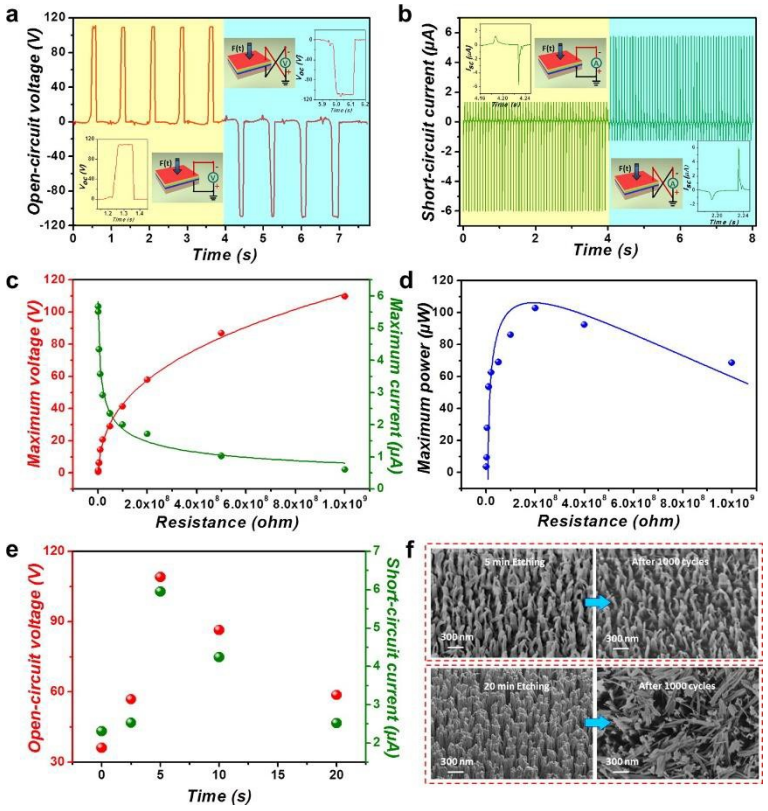

Figure. 7 Investigation on the performance of the generator with open-circuit voltage (a), short-circuit current (b), and electric output as a function of the load resistance (c). (d) Instantaneous electric power as a function of the load resistance. (e) The effect of time for etching polymer nanowires on open-circuit voltage and short-circuit current. (f) SEM images of the 1D Kapton nanowires. Reproduced with permission.[97] Copyright 2012, American Chemical Society.

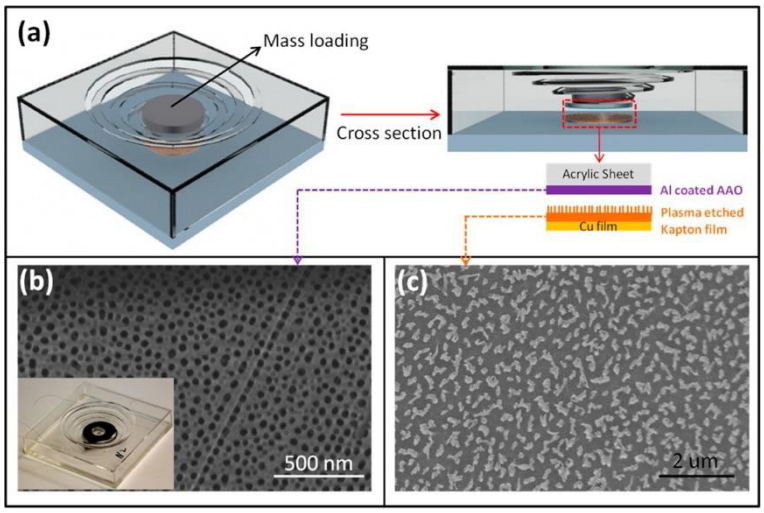

Figure. 8 TENG built on a suspended 3D spiral structure. (a) Schematic illustration of the TENG with cross-section view. SEM image of (b) anodic aluminum oxide and (c) 1D Kapton nanowires on the surface of Kapton film. The inset of (b) shows the real device. Reproduced with permission.[98] Copyright 2013, American Chemical Society.

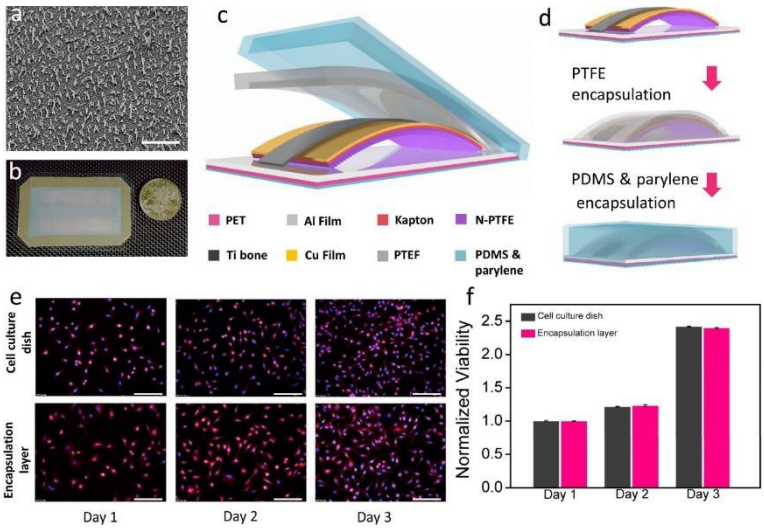

Figure. 9 Device structure, surface modification, and cytocompatibility of the iTENG. (a) SEM image of 1D PTFE nanowires on the surface of PTFE film (scale bar: 5 μm). (b) and (c) Schematic illustration of the iTENG. (d) Device encapsulation processes. (e) Fluorescence images of stained L929 cells cultured on the PDMS film which encapsulates the device (scale bar: 100 μm). (f) Cell viability after being cultured for 3 days. Reproduced with permission.[92] Copyright 2016, American Chemical Society.

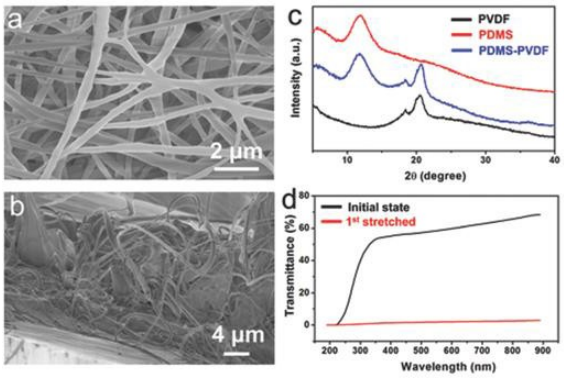

Figure. 10 (a) SEM image of PVDF nanowires. (b) Cross-section SEM image of PVDF nanowires in PDMS matrix. (c) XRD patterns of PVDF nanowires, PDMS, and the composite film. (d) Transmittance of the composite film. Reproduced with permission.[100] Copyright 2016, John Wiley & Sons.

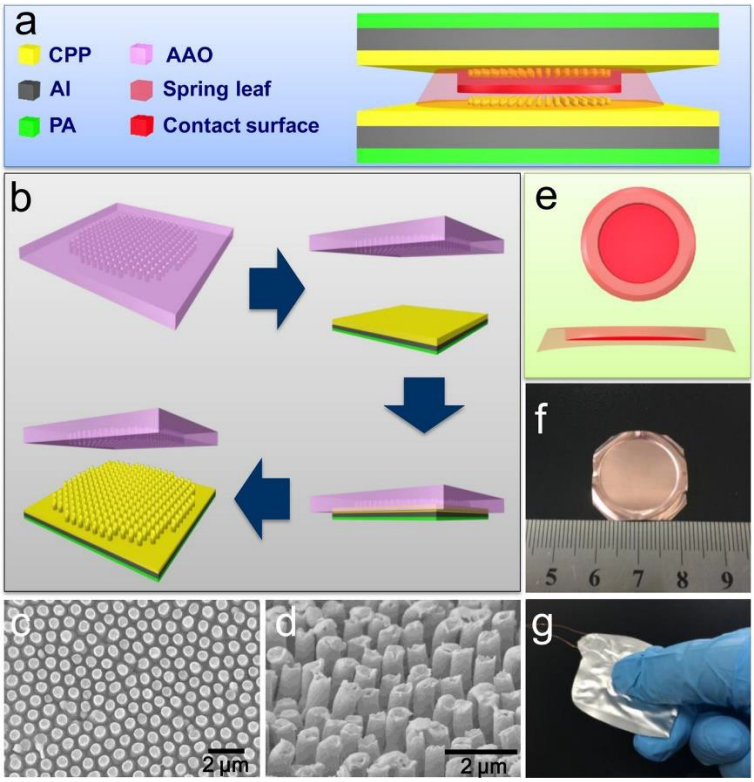

Figure. 11 (a) Schematic illustration of the TENG. (b) Fabrication processes of 1D PP nanopillar arrays on the surface. SEM images of (c) top view and (d) side view of 1D PP nanopillar. (e) and (f), Schematic illustration and optical photo of the cantilever spring leaf. (g) Real device of TES. Reproduced with permission.[69] Copyright 2016, American Chemical Society.

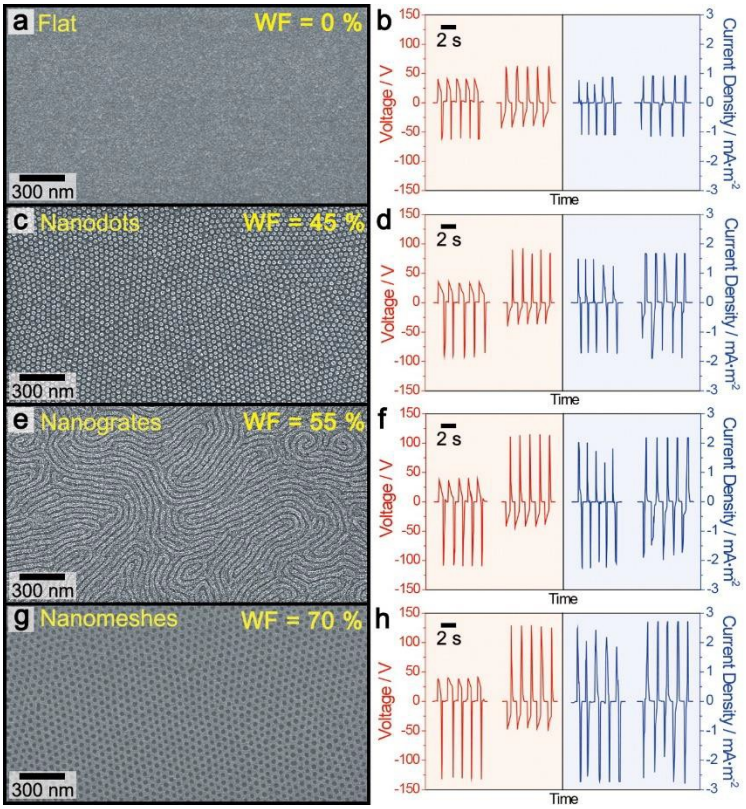

Figure. 12 SEM images of surface morphologies and the output signals of prepared TENGs: (a, b) TENG based on flat film, (c, d) TENG based on nanodots, (e, f) TENG based on 1D BCP nanogrates, and (g, h) TENG based on nanomeshes, respectively. Reproduced with permission.[101] Copyright 2014, American Chemical Society.

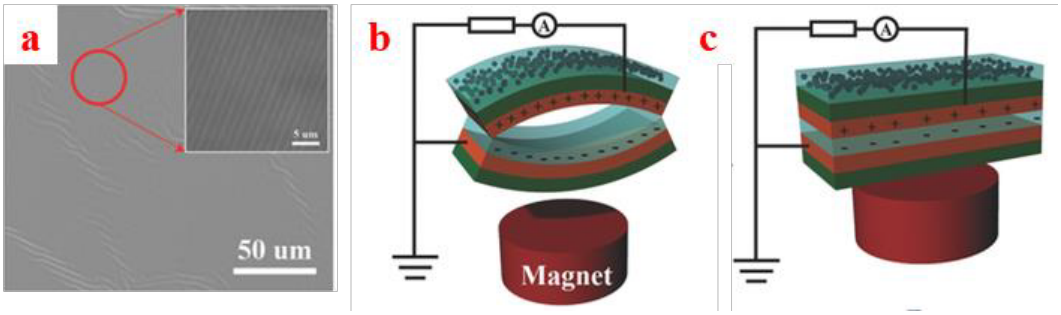

Figure. 13 (a) SEM image of the PDMS film with 1D PDMS microwires. (b) and (c), Schematic illustration of release and absorption state of magnetic-assistant noncontact TENG, respectively. Reproduced with permission.[105] Copyright 2016, John Wiley & Sons.

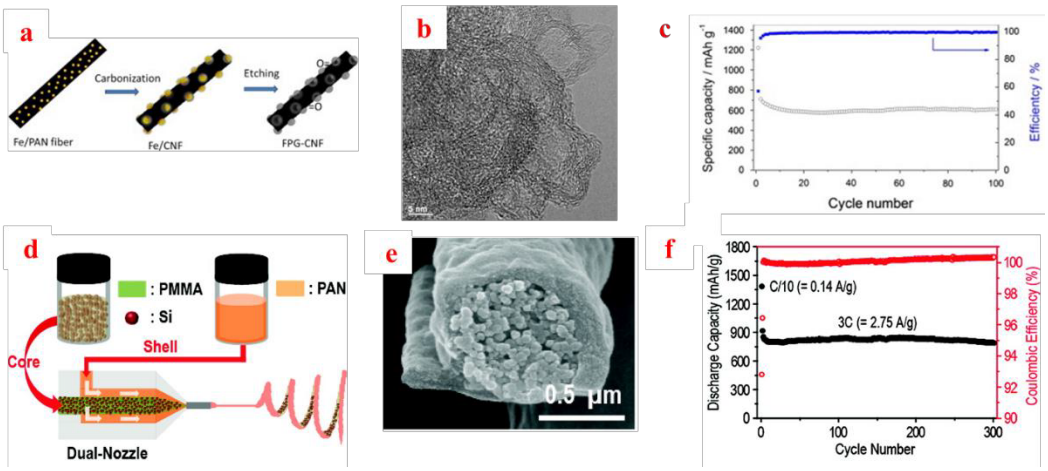

Figure. 14 (a) Evolution of functionalized, porous graphitic CNFs: Fe/PAN=electrospun PAN fibers with Fe particles before graphitization; Fe/CNF=CNFs with Fe_3C particles after graphitization; FPG-CNF=CNFs after etching with HNO_3 solution. (b) FPG-CNFs after removing Fe_3C particles. (c) Cyclic performance at 1000 mA g^{-1} of FPG-CNF electrodes.[122] (d) The electrospinning process using a dual nozzle. The PMMA solutions containing SiNPs and the PAN solution were injected into the core and shell channels of the nozzle, respectively. (e) A cross-sectional SEM view of a single SiNP@C indicating that the core full of Si NPs is wrapped by carbon shell. (f) Cycling performance of SiNP@C measured at 3C rate. Reproduced with permission.[109] Copyright 2012, American Chemical Society.

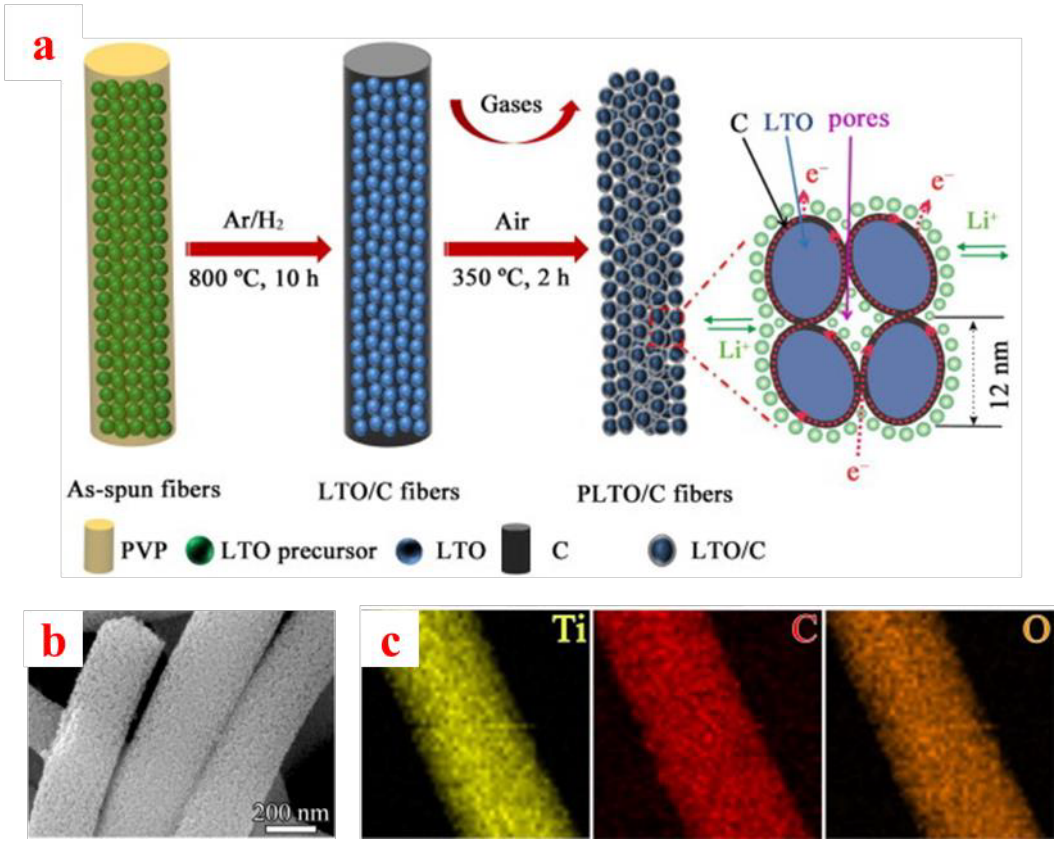

Figure. 15 (a) Schematic illustration of the formation of the PLTO/C nanofibers through electrospinning and a subsequent two-step heat-treatment. (b) PLTO/C nanofibers. (c) HAADF-STEM image and elemental mapping images of an individual fiber of PLTO/C. Reproduced with permission.[124] Copyright 2014, Elesiver.

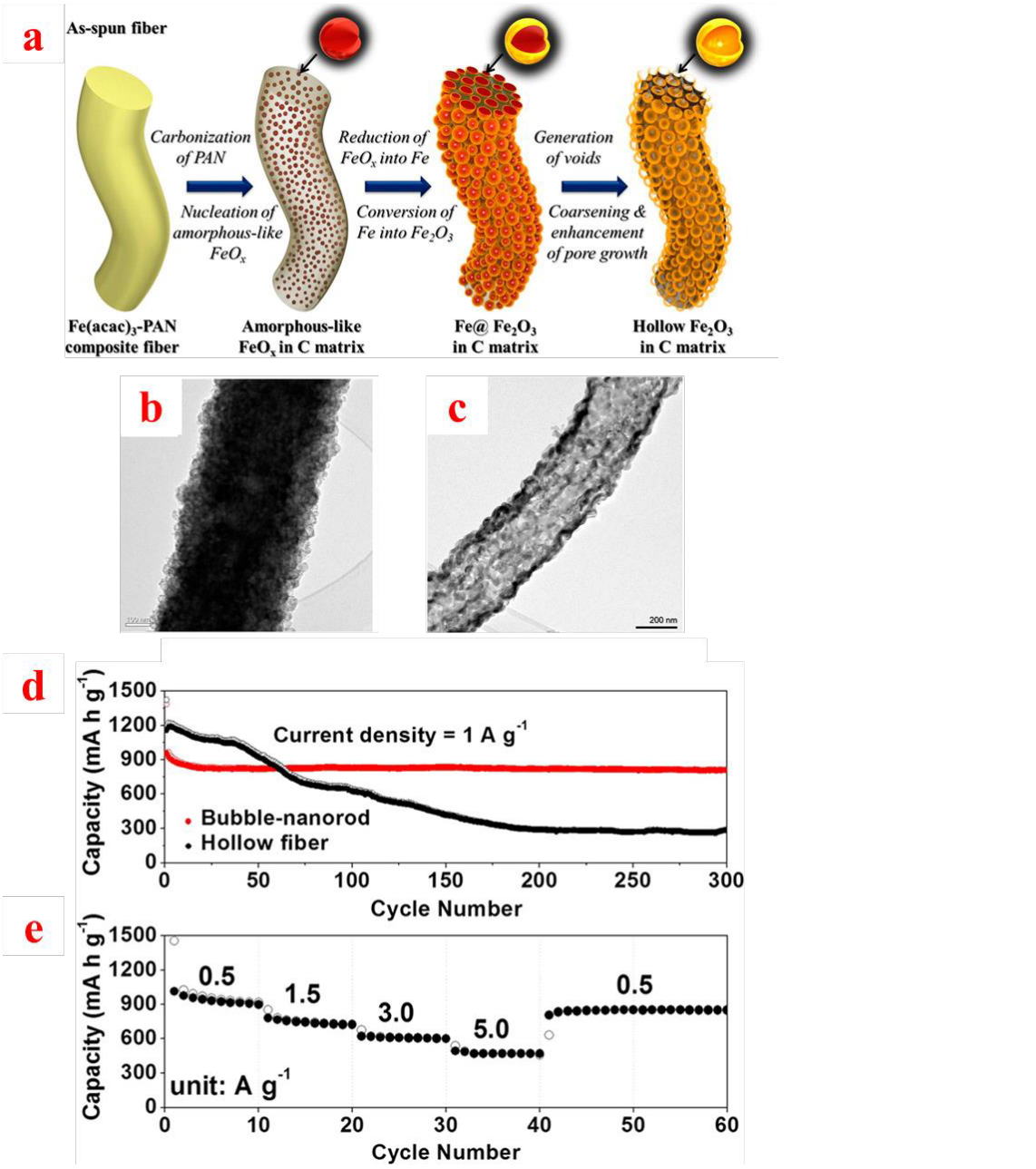

Figure. 16 (a) Formation mechanism of bubble-nanorod-structured Fe_2O_3-C composite nanofiber by Kirkendall-type diffusion. (b) TEM image of Fe_2O_3-C composite nanofibers. (c) TEM image of bare Fe_2O_3 hollow nanofibers formed by direct post-treatment of the electrospun nanofibers at 500 °C under air atmosphere. (d) Cycling performances, and (e) Rate performance of bubble-nanorod-structured

nanofibers. Reproduced with permission.[126] Copyright 2015, American Chemical Society.

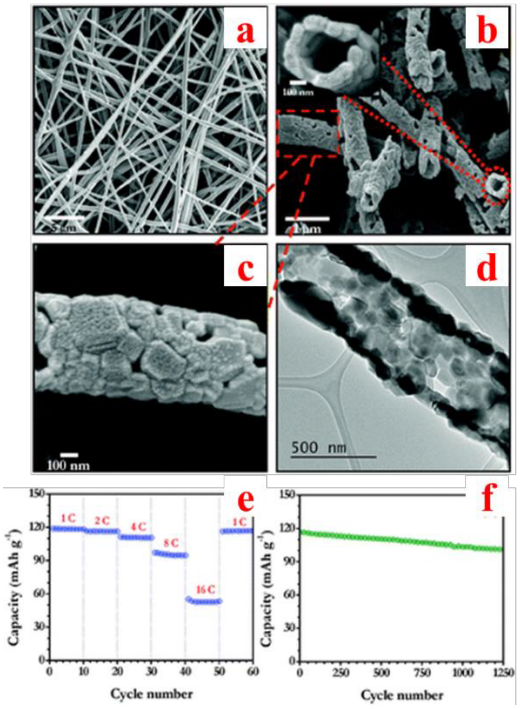

Figure. 17 (a) FESEM image of $LiMn_2O_4$ nanofibers fabricated by electrospinning method, (b) nanofibers after sintering at 800 °C for 5 h. Inset: magnified SEM image of hollow structure, (c) and (d) magnified SEM and TEM images of the single nanofibers, respectively. (e) rate performance studies and (f) long-term cyclability recorded between 3.5-4.3 V at a current density of 150 mA g^{-1}. Reproduced with permission.[137] Copyright 2013, RSC Publishing.

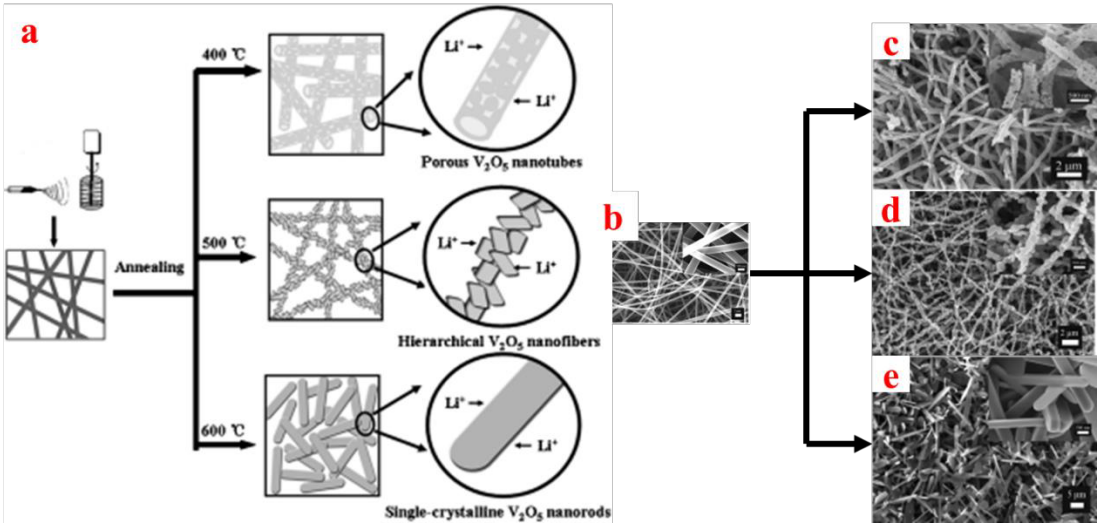

Figure. 18 (a) Preparation processes of V_2O_5 nanotubes, V_2O_5 nanofibers, and V_2O_5 nanobelts. (b) Electrospun precursor nanofibers and different V_2O_5 nanostructures (scale bar: 2 μm) after different annealing temperature at (c) 400 °C, (d) 500 °C, and (e) 600 °C. Reproduced with permission.[140] Copyright 2012, John Wiley & Sons..

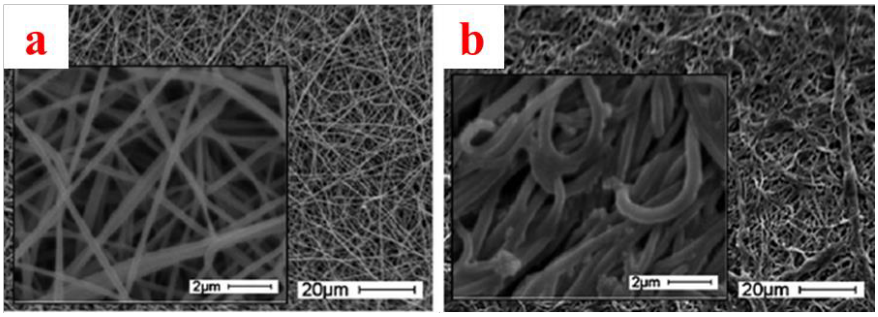

Figure. 19 SEM micrographs of the electrospun random mat (PVDF-10CTFE) before (a) and after (b) electrolyte (1M LiPF6 in EC/DMC 1:1) uptake. Reproduced with permission.[144] Copyright 2011, RSC Publishing.

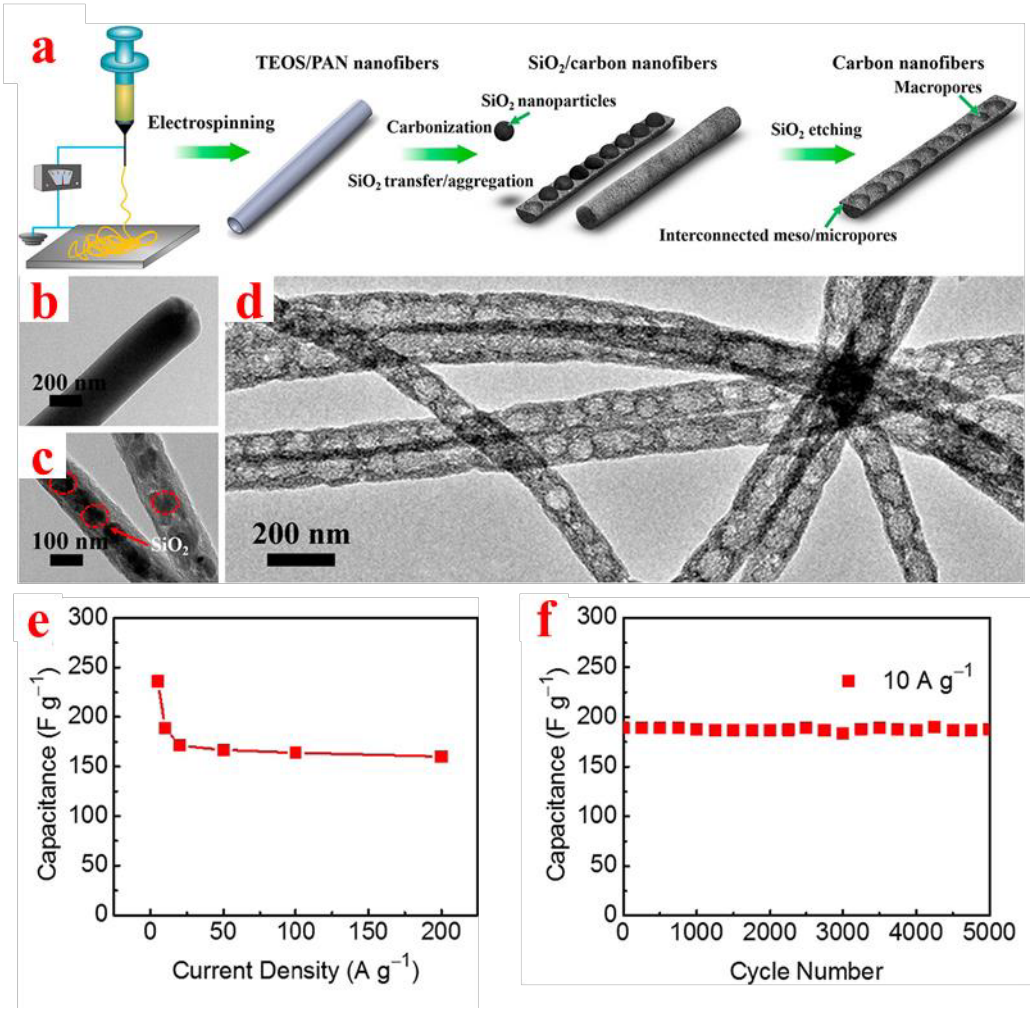

Figure. 20 Fabrication and characterization of the bamboo-like carbon nanofibers. (a) Schematic illustration of the fabrication processes of the bamboo-like carbon nanofibers. (b) TEM images of TEOS/PAN composite nanofibers, (c) TEM images of SiO_2/carbon composite nanofibers after carbonization, (d) TEM images of bamboo-like carbon nanofibers after removing SiO_2. (e) The specific capacitances at different current densities. (f) Cyclic stability of supercapacitor based on bamboo-like carbon nanofibers at a current density of 10 A/g. Reproduced with permission.[13] Copyright 2015, American Chemical Society.

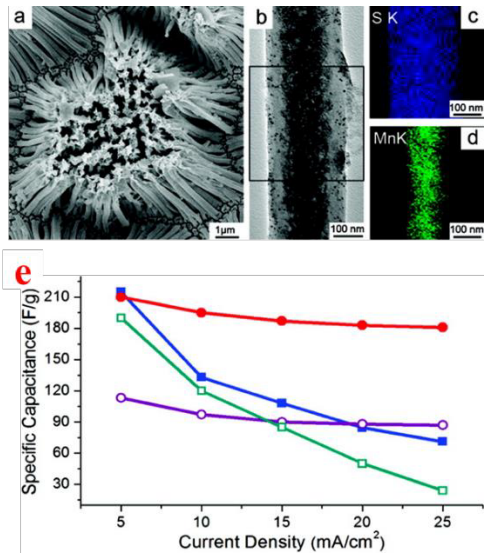

Figure. 21 (a and b) SEM and TEM images of MnO_2/PEDOT coaxial nanowires, respectively. (c and d) S and Mn elements mapping from EDS. (e) Specific capacitance of MnO_2 nanowires (closed blue square), PEDOT nanowires (open purple dots), MnO_2 thin film (open green square) and MnO_2/PEDOT coaxial nanowires (closed red dots) at difference charge/discharge current densities. Reproduced with permission.[24, 154] Copyright 2008, American Chemical Society.

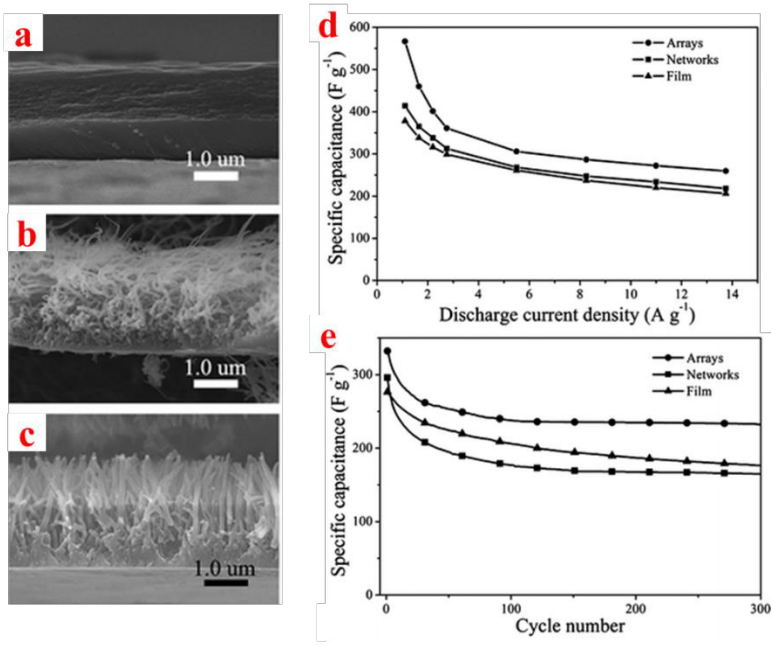

Figure. 22 Cross-sectional view of (a) PPy film, (b) NW networks, and (c) NW arrays. Their thicknesses were all controlled in the range of 2 to 2.5 μm. (d) Electrochemical measurement of PPy with different morphologies (Specific capacitances). Stability of PPy with different morphologies. (e) Capacitance versus cycle number for PPy film (£.), NW networks (■), and NW arrays (•) at a discharge current density of 2.75 A/g. Reproduced with permission.[156] Copyright 2010, RSC publishing.

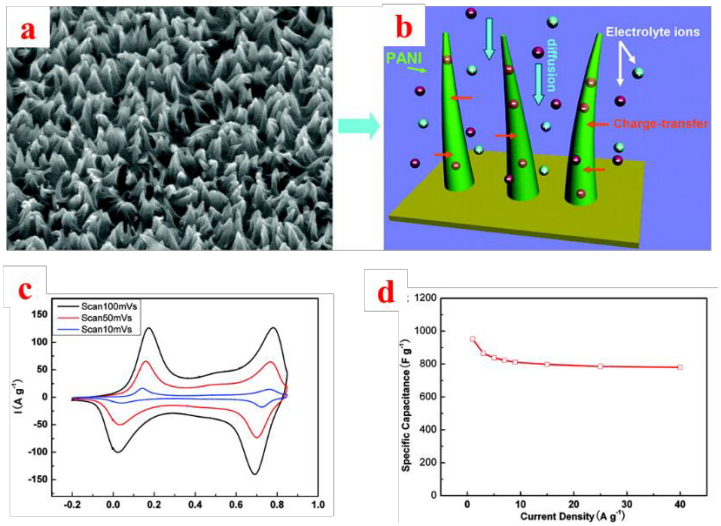

Figure. 23 (a) Top view SEM image of PAN nanowire arrays. (b) Schematic of the optimized ion diffusion path in nanowire arrays. (c) Cyclic voltammetry of PAN nanowire arrays at different scan rate in $HClO_4$ aqueous solution. (d) Specific capacitance measured at different current densities in $HClO_4$ aqueous solution. Reproduced with permission.[25] Copyright 2010, American Chemical Society.

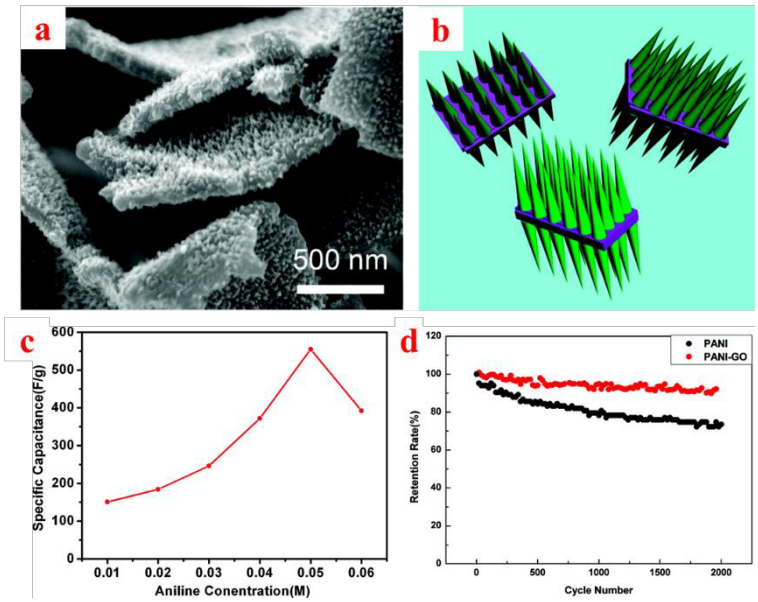

Figure. 24 (a) SEM images of PAN-GO samples; (b) Schematic illustration of PAN nanowires on the surface of GO sheets. (c) Influence of aniline concentration on the specific capacitance of PANI-GO. (d) Stability of supercapacitor based on PANI and PANI-GO. Reproduced with permission.[152] Copyright 2010, American Chemical Society.

Table 1. Fabrication methods for 1D polymer nanomaterials for energy device applications.

Techniques		Polymer materials	Feature size	Potential applications	Refs.
Electrospinning		polyaniline, polyimide, polyvinyl pyrrolidone, poly(vinyl alcohol), polybenzimidazole, phenolic resin, poly(vinyliden fluoride), cellulose	~ 100 nm	Nanogenerator; Lithium Ion Battery; Supercapacitor	[10, 13, 148]
Template-assisted		polypyrrole, poly(p-phenylenevinylene) and derivatives, polyaniline, polystyrene, polymethyl methacrylate, poly(3-hexylthiphene)	~ 20 nm	Nanogenerator; Polymer Solar cells; Lithium Ion Battery; Supercapacitor	[31] [57, 159-161] [162, 163] [49]
Template-free	Self-assembly	poly(3-hexylthiphene), polystyrene-block-polydimethylsiloxane	~5 nm	Nanogenerator; Polymer solar cells	[2, 7, 164]
	Electropolymerization	polypyrrole, polyaniline poly(3,4-ethylenedioxythiophene)	~ 5 nm	Supercapacitor	[23, 81]
Inductively Coupled Plasma		poly(3,4-ethylenedioxythiophene), polytetrafluoroethylene, poly(styrenesulfonate), ppy polypyrrole, poly(1-methyoxy-2-propyl acetate), polyvinylidene difluoride, poly(methyl-methacrylate), polystyrene (ps), poly(2-methoxy-5-2'-ethylhexyloxy)-(1,4-phenylenevinylene)	~ 20 nm	Nanogenerator	[165] [28, 29, 38, 88]

Table 2. The influence of different electrospinning parameters on the nanofiber diameter

Parameters	Influence on diameter of 1D polymer nanomaterials	Reference
Flow rate	Higher flow rate leads to increased diameter of 1D polymer nanomaterials	[48] [166]
Distance between needle and collector	Increment of distance between needle and collector tends to decrease the average diameter of 1D polymer nanomaterials	[48] [166] [167]
Concentration of polymer solution	Increment of concentration results in increment of diameter of 1D polymer nanomaterials	[167]
Applied voltage	Applied high voltage between needle and collector tends to result in larger diameter of 1D polymer nanomaterials	[168] [169]
Vapor diffusivity of solvent	Lower evaporating solvent leads to thinner fibers	[170]
Conductivity of polymer solution	Bigger diameter of 1D polymer nanomaterials are achieved by increasing polymer solution conductivity	[171]
Orifice radius	Decrement of orifice radius leads to smaller diameters of 1D polymer nanomaterials	[172]

Dr. Long-Biao Huang obtained B.Sc. and M.Sc. degree from the Xi'an Jiaotong University in 2004 and 2007, and then went to Global R&D center of Dow Chemical as Research Chemist. In 2014, He obtained his Ph.D. degree from Center Of Super-Diamond and Advanced Films (COSDAF) in City University of Hong Kong. He started his postdoctoral career in The Hong Kong Polytechnic University under supervision of Prof Jianhua Hao. He joined Shenzhen University as associate professor in College of Optoelectronic Engineering. His research interests include 1D polymer nanomaterials for different applications such as organic electronics, plasmonic and energy harvesting device.

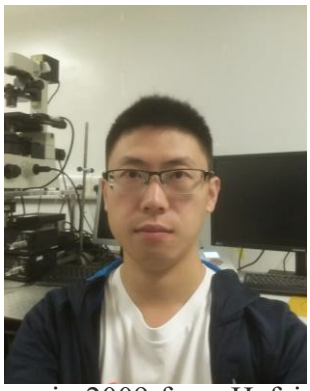

Mr. Wei Xu obtained his BSc degree in 2009 from Hefei University of technology. Then he received his Master degree in 2012 from Sichuan University. Now he is a PhD student in Department of Applied Physics under the supervision of Prof. Jianhua Hao. His current research interest is energy harvesting for self-powered system.

Prof. Jianhua Hao obtained his BSc, MSc and PhD at Huazhong University of Science and Technology, China. After working at Penn State University, USA, University of Guelph, Canada and the University of Hong Kong, Jianhua Hao joined the faculty in the Hong Kong Polytechnic University (PolyU) in 2006. He is currently a Professor and Associate Head of the Department of Applied Physics in PolyU. Jianhua Hao has published more than 210

papers indexed by ISI Web of Science. His research interests include metal-ion doped luminescent materials and devices, functional thin-films, two-dimensional materials and heterostructures, piezophotonics and nanogenerator.

Table of Content: 1D polymer nanomaterials with the merits of nanointerface, high surface area and porous structure have widely been applied to improve the performances of advanced energy devices. Herein, we summarize the representative fabrication methods of 1D polymer nanomaterials in combination with overviews of typical energy devices, including nanogenerator, lithium ion battery and supercapacitor.

Keyword: 1D polymer nanomaterials, nanogenerators, battery, supercapacitor, energy device

L.-B. Huang, W. Xu, J. Hao*

Title: Energy Device Applications of Synthesized 1D Polymer Nanomaterials